Virial expansions for quantum plasmas: Diagrammatic resummations

Angel Alastuey,[1] Francoise Cornu,[2] and Asher Perez[1]
[1]*Laboratoire de Physique, Ecole Normale Supérieure de Lyon, 69364 Lyon 07, France*
[2]*Laboratoire de Physique Théorique–ENSLAPP, Ecole Normale Supérieure de Lyon, 69364 Lyon 07, France*
(Received 26 July 1993)

We are studying the equilibrium properties of quantum Coulomb fluids in the low-density limit. In the present paper, we only consider Maxwell-Boltzmann statistics. Use of the Feynman-Kac path-integral representation leads to the introduction of an equivalent classical system made of filaments interacting via two-body forces. All the corresponding Mayer-like graphs diverge because of the long-range Coulombic nature of the filament-filament potential. Inspired by the work of Meeron [J. Chem. Phys. **28**, 630 (1958); *Plasma Physics* (McGraw-Hill, New York, 1961)] for purely classical systems, we show that these long-range divergencies can be resummed in a systematic way. We then obtain a formal diagrammatic representation for the particle correlations of the genuine quantum system. The prototype graphs in these series are made of root and internal filaments, connected by two-body resummed bonds according to well-defined topological rules. The resummed bonds depend on the particle densities and decay faster than the bare Coulomb potential because of screening. Some bonds decay algebraically as $1/r^3$ in accord with the absence of exponential clustering, while the other ones are short ranged. This ensures the integrability of all the above prototype graphs. Moreover, we show that the filament densities, which are the statistical weights of the filaments in these graphs, can themselves be calculated in terms of the particle densities via a well-behaved diagrammatic series. This provides a useful algorithm for expanding the Maxwell-Boltzmann thermodynamic functions in powers of the particle densities, as to be described in a second future paper. The exchange effects due to Fermi or Bose statistics will be considered in a third paper.

PACS number(s): 05.30.−d, 05.70.Ce, 52.25.Kn

I. INTRODUCTION

A description of matter in terms of a quantum fluid made of electrons and nuclei interacting via Coulomb forces is of fundamental importance for many physical situations where a nonvanishing fraction of free charges appears. For instance, this occurs in various astrophysical objects (such as the sun or white dwarfs) and in the laboratory plasmas used in confinement experiments. In this context, the study of the equilibrium properties of a quantum Coulomb fluid is useful for both understanding the structure of the above systems and analyzing the observational data (for instance, those from helioseismology). Such a study is also of conceptual interest in understanding states of matter where only neutral atomic or molecular entities exist. In this spirit, we mention the beautiful work by Fefferman [1], who rigorously showed that, in some low-temperature and low-density limit, electrons and protons form a gas of hydrogen atoms. The physical conditions on the Earth are far from this scaling limit and favor the presence of molecular hydrogen.

The purpose of this series of papers is to propose systematic prescriptions for calculating the low-density expansions (at fixed temperature) of equilibrium quantities in quantum Coulomb fluids. For systems with short-range forces, the familiar Mayer expansion [2] used in classical statistical mechanics has finite coefficients and can be extended to the quantum case [3] by introducing the Feynman-Kac path-integral representation [4]. For classical Coulomb systems, all the Mayer graphs diverge because of the long-range (nonintegrable) nature of the Coulomb potential $v_c(r)=1/r$ (moreover in the classical case the Coulomb potential is regularized at short distances in order to avoid the collapse between opposite charges). As first noticed by Mayer [5] and Salpeter [6], these long-range (infrared) divergencies can be eliminated by resumming all the convolution chains built with the Coulomb potential. This mathematical recipe reflects screening, a many-body (collective) effect discovered independently by Gouy [7], Chapman [8], and Debye and Hückel [9]. Meeron [10] and Abe [11] have shown that the chain resummation leads to a new class of graphs built with short-range bonds. Our main point is to extend the Abe-Meeron procedure to the quantum case. We show that the series of divergent graphs in the Feynman-Kac representation can be reorganized in a series of finite resummed graphs. This provides a useful algorithm for calculating density expansions, where various physical effects such as screening, diffraction, formation of atomic or molecular entities, and statistics are treated in a simultaneous and coherent way.

In the literature, to our knowledge, there exist two attempts to derive low-density expansions for quantum plasmas. First, Ebeling [12] has applied Morita's idea which consists in introducing classical equivalent systems with two-, three-, and higher-order many-body effective interactions. The two-body effective potential between two charges is essentially defined as the logarithm of the symmetrized density matrix associated with the two-body Hamiltonian of these charges. Similarly, the N-body

effective potentials ($N>2$) are defined recursively in terms of the matrix elements of the N-body quantum Gibbs factors and of the lower-order effective potentials. In practice, only two-body effective potentials have been retained [13,14]. This amounts to considering well-behaved classical systems with two-body Coulomb interactions that are regularized at short distances [quantum effects smooth out the singularity of $v_c(r)$ at the origin]. The contributions of the three-body and higher-order interactions are expected to be at least of order ρ^3, where ρ is a generic notation for particle densities. The main drawback of this formalism is precisely the absence of a detailed control of these contributions. Second, Rogers [15] started with the standard quantum many-body perturbative expansions with respect to the interaction potential v_c in the framework of the grand-canonical ensemble. These expansions can be written in terms of graphs similar to those which appear in field theory [16], where fermionic or bosonic loops associated with imaginary-time free propagators are connected at different times by an arbitrary number of interaction lines v_c. The long-range Coulomb divergencies are eliminated via the well-known ring resummations [17]. Rogers proposed a classical treatment of these resummations combined with a reorganization of the series in v_c in order to introduce Coulomb thermal propagators at short distances. In this procedure, some terms are left over since they are expected to be quantitatively small in the physical regimes considered by the author (i.e., at moderately high densities where complex entities made of several charges may be formed).

In Sec. II, we define the model $\mathcal{S}$. It is made of point particles with mass m_α, carrying a charge e_α, and a spin σ_α; α is a species index which specifies the nature of the particle (for instance, electron or proton in the case of the hydrogen plasma). Its Hamiltonian is purely Coulombic, i.e., it involves only two-body Coulomb interactions of the form $e_\alpha e_\beta v_c(r)$. This Hamiltonian is nonrelativistic and does not depend on the spins. Lieb and Lebowitz [18] have shown that the present model has a well-behaved thermodynamic limit if and only if at least one species obeys Fermi statistics. Since the thermodynamic and correlation functions for the bulk are then well-defined intrinsic quantities, we will formally carry out the diagrammatic resummations in an infinite volume. In principle, there is no need to explicitly consider boundary effects which should disappear in the thermodynamic limit. Furthermore, although Fermi statistics are crucial for avoiding the collapse of all matter into a macroscopic molecule, the density expansions are term by term well behaved in the framework of Maxwell-Boltzmann (MB) statistics. This is because disregarding the many-body collective effect which induces screening, the contributions at a given order in the density involve a finite number of charges. Moreover use of the Slater sums provides a natural perturbative representation of the exchange contributions, where the reference system is described by MB statistics. These circumstances allow us to proceed as follows. First, in the present paper, we only consider MB statistics and we derive a formal diagrammatic representation of the particle correlations where the long-range Coulomb divergencies are resummed. The corresponding density expansions of the MB thermodynamic functions will be studied in a second paper; each term of these representations is finite, but the whole series should diverge in agreement with the instability of the MB system. The exchange effects associated with Fermi and Bose statistics will be dealt with in a third paper.

We turn to the Feynman-Kac representation with MB statistics in Sec. III. For the sake of pedagogy, we first expose how the so-called Feynman-Kac (FK) formula is inferred from the Feynman path integral for the thermal propagator of one particle in an external potential. The application of this formula to the MB N-body density matrix of $\mathcal{S}$ leads, in a very natural way, to the introduction of an auxiliary classical system $\mathcal{S}^*$ made of closed filaments (also called "polymers" in the literature [19]). Since the filaments still interact via two-body forces, the equilibrium quantities of $\mathcal{S}^*$, and consequently those of $\mathcal{S}^{\mathrm{MB}}$, can be represented by series of Mayer-like graphs where the familiar points are replaced here by extended objects.

The interaction potential between two filaments decays as the Coulomb potential itself at large distances. Thus all the above Mayer graphs for $\mathcal{S}^*$ diverge and the situation is analogous to what happens for classical Coulomb systems. In Sec. IV, we show that these long-range divergencies can be eliminated by resumming the convolution chains, as in the classical case. In fact, inspired by the works by Meeron [10] and Abe [11], we transform the whole set of Mayer graphs defining the two-body correlations of $\mathcal{S}^*$ into a new set of finite resummed graphs with the same topological structure. The new graphs are built with four kinds of resummed bonds where the summation of the Coulomb convolution chains makes the familiar Debye potential appear in a natural way. Two of these bonds are short ranged and proportional to the charge-charge and dipole-charge Debye screened potentials respectively (the charges and the dipoles are those carried by the filaments). On the other hand, the third and fourth bonds decay only as $1/r^3$ at large distances. Although this power law is at the border line for integrability, the resummed graphs are indeed finite because they are sufficiently connected. Therefore the screening mechanism which eliminates the long-range divergencies is the same one as in the classical case. However, it is not as efficient since some resummed bonds still decay algebraically. These slow decays should ultimately pollute the correlations with algebraic tails in agreement with the predictions of Refs. [20] and [21]: the effective multipole potentials induced by quantum fluctuations cannot be exponentially screened.

The statistical weights in the above graphs are the filament densities $\rho(\mathcal{E})$ which depend on the shape of the filaments in a complicated way. In Sec. V, we study the functional $\rho(\mathcal{E})$, by starting from its grand-canonical representation in terms of fugacities. The long-range Coulomb divergencies in the corresponding Mayer-like diagrams are resummed by a scheme similar to that used in Sec. IV. This provides a well-behaved diagrammatic representation of $\rho(\mathcal{E})$, from which we infer the structure of the small-fugacity expansion of this functional. Elim-

inating the fugacities in favor of particle densities, we then show that $\rho(\mathcal{E})$ can be represented by a double integer series in $\rho^{1/2}$ and $\ln\rho$. The first terms of this expansion are calculated up to order ρ^2.

The resummed diagrammatic representation of the particle correlations, combined with the particle-density expansion of the functional $\rho(\mathcal{E})$, allow calculation of any thermodynamic function, to be described in the second paper of this series. In the third paper, we shall evaluate the exchange contributions and give the final form of the density expansions for Bose and Fermi statistics. We shall then comment and compare with other theories. In the meantime, we mention that part of the present work has been announced previously [22].

II. MODEL

A. Definitions: Grand-canonical ensemble

We consider a multicomponent system $\mathcal{S}$ made of point charges e_α with mass m_α and spin σ_α. The species index α specifies the nature of the particle which will be either an electron or a nucleus in mot applications. To ensure charge neutrality, there are at least two species of charge which are positive and negative respectively. The charges are assumed to interact via the two-body Coulomb potential, which reads $e_\alpha e_\beta/r$ for two charges e_α and e_β separated by a distance r. The corresponding Hamiltonian for N charges enclosed in a box with volume Λ is

$$H_{N,\Lambda}=-\sum_i \frac{\hbar^2}{2m_i}\Delta_i+\frac{1}{2}\sum_{\substack{i,j\\ i\neq j}}\frac{e_i e_j}{|\mathbf{r}_i-\mathbf{r}_j|}\ , \tag{2.1}$$

where $i=\begin{bmatrix}k\\ \alpha\end{bmatrix}$ is a double index; k runs from 1 to the number N_α of charges of species α and α runs from 1 to the number n_s of species (the total particles number $N=\sum_\alpha N_\alpha$). The boundary conditions which define $H_{N,\Lambda}$ are of the Dirichlet type, i.e., the eigenfunctions of $H_{N,\Lambda}$ vanish at the surface of the box.

Let the system be in thermal equilibrium at temperature T ($\beta=1/k_B T$). The grand-partition function of the finite system reads

$$\Xi_\Lambda=\mathrm{Tr}_\Lambda\exp\left[-\beta\left[H_{N,\Lambda}-\sum_\alpha \mu_\alpha N_\alpha\right]\right], \tag{2.2}$$

where μ_α is the chemical potential of species α. In the definition (2.2), the trace Tr_Λ runs over all the states satisfying the above boundary conditions and symmetrized according to the statistics of each species. Note that the total charge $\sum_\alpha N_\alpha e_\alpha$ carried by each of these states may be different from zero.

B. The thermodynamic limit

Lieb and Lebowitz [18] have shown that the thermodynamic limit (TL) of the present system exists if and only if at least one species obeys Fermi statistics. The TL is defined as the infinite volume limit ($\Lambda\to\infty$), while the chemical potential μ_α and the temperature T are kept fixed. The above theorem means that the thermodynamic quantities relative to the infinite system have the right extensive properties. In particular, the bulk pressure P given through

$$\beta P=\lim_{\mathrm{TL}}\frac{1}{\Lambda}\ln\Xi_\Lambda \tag{2.3}$$

is a well-behaved function of the intensive parameters μ_α and β which does not depend on the shapes of the finite boxes considered in the TL. If the fugacities $z_\alpha=\exp(\beta\mu_\alpha)$ are small enough (at a given temperature), the system surely is in a fluid phase. The local density of any species α then becomes uniform in the TL and reduces to

$$\rho_\alpha=z_\alpha\frac{\partial}{\partial z_\alpha}\left[\lim_{\mathrm{TL}}\frac{1}{\Lambda}\ln\Xi_\Lambda\right]\Bigg|_\beta . \tag{2.4}$$

Furthermore, the infinite system is locally neutral, i.e.,

$$\sum_\alpha e_\alpha\rho_\alpha=0 \tag{2.5}$$

for any set of the fugacities. This is due to the fact that all the excess charges associated with non-neutral states ($\sum_\alpha e_\alpha N_\alpha\neq 0$) go to the boundaries in order to minimize the electrostatic energy. Once the TL has been taken, these charges are rejected to infinity and the bulk region is neutral [23].

The existence of the TL is guaranteed by the combination of several phenomena. First, the most probable microscopic configurations can be organized in sets of finite neutral clusters which are weakly coupled because of screening. This physical idea can be formulated in a precise mathematical way, with the help of the "cheese theorem" and of the harmonicity of the Coulomb potential [24]. Of course, this screening mechanism requires the presence of charges of opposite signs (otherwise the system explodes). Second, the classical collapse between two opposite charges at short distances is avoided by the uncertainty principle. The latter ensures that the quantum density matrix remains finite, and consequently integrable, at zero separations in configuration space. Third, the H stability prevents the macroscopic collapse of all the matter into a big molecule. This property stipulates that the Hamiltonian H_N in the finite volume is bounded below by an extensive constant (i.e., the ground state of H_N is bounded below by $Cst\times N$). Dyson and Lenard [25] have proved that the H stability is enforced by Pauli principle, which requires the presence of fermions.

In this series of papers, we are interested in bulk properties of the infinite system. Since the TL exists, it is reasonable to assume that the corresponding quantities can be obtained without any explicit consideration of boundary effects. Therefore, from now on, we shall perform all calculations in the infinite volume.

C. Maxwell-Boltzmann statistics

On the right-hand side of (2.2), the trace can be taken over the symmetrized states $|\mathbf{R}_N\sigma_N^z\rangle_S$ in configuration and spin spaces, defined via the usual Slater sums,

$$|\mathbf{R}_N\sigma_N^z\rangle_S=\frac{1}{\prod_\alpha (N_\alpha!)^{1/2}}\sum_{\mathcal{P}_\alpha}\prod_\alpha \epsilon_\alpha(\mathcal{P}_\alpha)\otimes_i|\mathbf{r}_{\mathcal{P}_\alpha(i)}\sigma^z_{\mathcal{P}_\alpha(i)}\rangle\ . \tag{2.6}$$

In (2.6), $\mathcal{P}_\alpha$ is a permutation of $(1,\ldots,N_\alpha)$, $\mathcal{P}_\alpha(i)=(\mathcal{P}_\alpha(k),\alpha)$ and $\epsilon_\alpha(\mathcal{P}_\alpha)$ is either 1 if the particles of species α are bosons (σ_α integer) or the signature (±1) of $\mathcal{P}_\alpha$ in the fermionic case (σ_α half integer). Furthermore $\otimes_i$ means the tensorial product over the one-body states $|\mathbf{r}\sigma^z\rangle$ describing a particle localized at $\mathbf{r}$ with the projection of its spin along a given z axis equal to σ^z [σ^z may take $(2\sigma_\alpha+1)$ values]. Using (2.6), we obtain

$$\Xi_\Lambda=\sum_{N_\alpha=0}^{\infty}\frac{\prod_\alpha z_\alpha^{N_\alpha}}{\left[\prod_\alpha (N_\alpha!)\right]^2}\sum_{\mathcal{P}_\alpha,\mathcal{P}'_\alpha}\prod_\alpha\epsilon_\alpha(\mathcal{P}_\alpha)\epsilon_\alpha(\mathcal{P}'_\alpha)\sum_{\{\sigma_i^z\}}\prod_i\langle\sigma^z_{\mathcal{P}'_\alpha(i)}|\sigma^z_{\mathcal{P}_\alpha(i)}\rangle\int_{\Lambda^N}\prod_i d\mathbf{r}_i\langle\mathbf{r}_{\mathcal{P}'_\alpha(i)}|\otimes_i|\exp(-\beta H_{N,\Lambda})|\otimes_i|\mathbf{r}_{\mathcal{P}_\alpha(i)}\rangle\ . \tag{2.7}$$

Since the Hamiltonian $H_{N,\Lambda}$ does not depend on the spins, the spin part of the matrix elements factorizes and contributes the trivial degeneracy factor $\sum_{\{\sigma_i^z\}}\prod_i\langle\sigma^z_{\mathcal{P}'_\alpha(i)}|\sigma^z_{\mathcal{P}_\alpha(i)}\rangle$ which only depends on the pairs of permutations $(\mathcal{P}_\alpha,\mathcal{P}'_\alpha)$.

The Slater-sum representation (2.7) of Ξ_Λ provides a natural perturbative scheme for treating the exchange effects associated with Fermi or Bose statistics. Indeed, the "square" terms ($\mathcal{P}_\alpha=\mathcal{P}'_\alpha$ for any α), where the diagonal matrix elements of $\exp(-\beta H_{N,\Lambda})$ in configuration space appear, obviously correspond to MB statistics. A "rectangle" term ($\mathcal{P}_\alpha\neq\mathcal{P}'_\alpha$ for at least one species) involves the exchange of n particles ($n\geq2$). The corresponding matrix elements of $\exp(-\beta H_{N,\Lambda})$ are off diagonal with respect to the positions of the n exchanged particles. Since these nondiagonal parts are short ranged, the contribution of the above rectangle term is at least of order ρ^n (roughly speaking, a cyclic permutation of p particles of species α amounts to replacing them by one effective particle with fugacity z_α^p). The reorganization of the representation (2.7) with respect to the number n of exchanged particles then appears quite suitable for the purpose of calculating low-density expansions. Since the $(N-n)$ particles, which are not involved in the exchange, are described by MB statistics, the MB system turns to be the natural reference system in this perturbative evaluation of the exchange effects. In the first two papers, we will study the MB reference system, while the exchange effects will be considered in the third paper.

The MB grand-partition function $\Xi_\Lambda^{\mathrm{MB}}$ follows directly from the representation (2.7) by keeping only the square terms $\mathcal{P}_\alpha=\mathcal{P}'_\alpha$. For each species α, the spin-degeneracy factor reduces to $(2\sigma_\alpha+1)^{N_\alpha}$; the contributions of all the permutations $\mathcal{P}_\alpha$ are identical to that of the identity and lead to the multiplicative factor $N_\alpha!$. We then recover the standard expression

$$\Xi_\Lambda^{\mathrm{MB}}=\sum_{N_\alpha=0}^{\infty}\prod_\alpha\frac{z_\alpha^{N_\alpha}}{N_\alpha!}(2\sigma_\alpha+1)^{N_\alpha}\times\int_{\Lambda^N}\prod_i d\mathbf{r}_i\langle\mathbf{R}_N|\exp(-\beta H_{N,\Lambda})|\mathbf{R}_N\rangle \tag{2.8}$$

with $|\mathbf{R}_N\rangle=\otimes_i|\mathbf{r}_i\rangle$. Because of the absence of H stability with MB statistics, the TL of $(\ln\Xi_\Lambda^{\mathrm{MB}})/\Lambda$ does not exist. However, we shall see that the MB equilibrium quantities of the infinite system can be formally represented by their density expansions which remain term-to-term well behaved. Indeed, the MB macroscopic instability does not cause any short-range divergency in the viral coefficients which involve a finite number N of particles. It only affects the behavior of these coefficients in the large-N limit and should, in principle, prevent the convergence of the corresponding series.

III. THE FEYNMAN-KAC REPRESENTATION

A. The case of one particle

For the sake of pedagogy, we first illustrate the Feynman-Kac representation for one particle with mass m submitted to an external potential $V(\mathbf{r})$. According to the original path integral formulation introduced by Feynman and Hibbs [26], the diagonal matrix element of $\exp\{-\beta[-(\hbar^2/2m)\Delta+V]\}$ reads

$$\left\langle\mathbf{r}\left|\exp\left[-\beta\left[-\frac{\hbar^2}{2m}\Delta+V\right]\right]\right|\mathbf{r}\right\rangle=\sum_{(\text{all paths})}\exp\left[-\frac{S(\mathbf{r}(t))}{\hbar}\right], \tag{3.1}$$

where $S(\mathbf{r}(t))$ is the classical action in the potential $-V$,

$$S(\mathbf{r}(t))=\int_0^{\beta\hbar}dt\left\{\frac{m}{2}\left[\frac{d\mathbf{r}(t)}{dt}\right]^2+V(\mathbf{r}(t))\right\} \tag{3.2}$$

for a path $\mathbf{r}(t)$ going from $\mathbf{r}$ to $\mathbf{r}$ in a "time" $\beta\hbar$. The summation in (3.1) runs over all such paths. The adjective "genuine" will be used to refer to this direct formulation of the problem. In (3.1) and (3.2), the variable changes $t=s\beta\hbar$ and $\mathbf{r}(t)=\mathbf{r}+\lambda\boldsymbol{\xi}(s)$, with $\lambda=(\beta\hbar^2/m)^{1/2}$ the de Broglie thermal wavelength, lead to the so-called Feynman-Kac representation [4]

$$\left\langle \mathbf{r}\left|\exp\left[-\beta\left[-\frac{\hbar^2}{2m}\Delta+V\right]\right]\right|\mathbf{r}\right\rangle = \frac{1}{(2\pi\lambda^2)^{3/2}}\int \mathcal{D}(\xi)\exp[-\beta V^*(\mathbf{r},\xi)] \quad (3.3)$$

with

$$V^*(\mathbf{r},\xi)=\int_0^1 ds\, V(\mathbf{r}+\lambda\xi(s)) \ . \quad (3.4)$$

The factor $\exp[-\beta V^*(\mathbf{r},\xi)]$ obviously arises from the potential part of the action S. The corresponding kinetic factor, i.e., $\exp\{-\frac{1}{2}\int_0^1 ds[d\xi(s)/ds]^2\}$, is absorbed in the normalized Gaussian measure $\mathcal{D}(\xi)$ which defines the functional integration over all the dimensionless Brownian bridges $\xi(s)$ subjected to the constraints $\xi(0)=\xi(1)=\mathbf{0}$. This measure is intrinsic, i.e., independent of all the physical parameters, and its covariance is given by

$$\int \mathcal{D}(\xi)\xi_\mu(s)\xi_\nu(t)=\delta_{\mu\nu}\times \begin{cases} s(1-t), & s\le t \\ t(1-s), & t\le s \end{cases} \quad (3.5)$$

where ξ_μ is the component of ξ along the μ axis. It is very natural to interpret $\exp[-\beta V^*(\mathbf{r},\xi)]$ as the Boltzmann factor corresponding to a classical closed filament located at $\mathbf{r}$ and with a shape parameterized by $\lambda\xi(s)$. The potential V^* seen by this filament is the average of the genuine potential seen by the particle when it runs along the curve $\mathbf{r}+\lambda\xi(s)$. The Feynman-Kac representation (3.3) stipulates that the Gibbs factor for the quantum point particle exactly reduces to the shape average of this Boltzmann factor with the Gaussian measure $\mathcal{D}(\xi)$. The de Broglie wavelength λ controls the characteristic size of a filament: roughly speaking, the statistical weight of a filament with size R behaves as $\exp(-R^2/\lambda^2)$. Note that the classical limit of the density matrix is immediately obtained from (3.3) by replacing $V^*(\mathbf{r},\xi)$ by $V(\mathbf{r})$: in this limit, λ goes to zero and the spatial extent of the filaments can be neglected in the calculation of $V^*(\mathbf{r},\xi)$.

B. The auxiliary system $\mathcal{S}^*$

Similarly to the expression (3.3), the FK representation of the diagonal matrix element of $\exp(-\beta H_{N,\Lambda})$ reads

$$\langle \mathbf{R}_N|\exp(-\beta H_{N,\Lambda})|\mathbf{R}_N\rangle = \prod_\alpha \frac{1}{(2\pi\lambda_\alpha^2)^{3N_\alpha/2}}\int \prod_i \mathcal{D}(\xi_i)\exp\left[-\frac{\beta}{2}\sum_{\substack{i,j\\ i\neq j}} e_i e_j \int_0^1 ds\, v_c(|\mathbf{r}_i+\lambda_i\xi_i(s)-\mathbf{r}_j-\lambda_j\xi_j(s)|)\right] , \quad (3.6)$$

where each Brownian bridge $\xi_i(s)$ parameterizes the trajectory of the ith particle in the genuine Feynman path integral and is distributed according to the intrinsic Gaussian measure defined above. This representation suggests introducing the following auxiliary classical system $\mathcal{S}^*$ made of closed filaments interacting via two-body forces. Each filament is characterized by its spatial position $\mathbf{r}$ and two internal degrees of freedom, the dimensionless path $\xi(s)$ associated with its shape and the species index α which specifies its spatial extension λ_α and the strength e_α of its coupling with the other filaments. We denote by $\mathcal{E}\equiv(\alpha,\mathbf{r},\xi)$ the state of such a filament. Two filaments in states $\mathcal{E}$ and $\mathcal{E}'$ interact via the two-body potential $e_\alpha e_{\alpha'} v(\mathcal{E},\mathcal{E}')$ with

$$v(\mathcal{E},\mathcal{E}')=\int_0^1 ds\, v_c(|\mathbf{r}+\lambda_\alpha\xi(s)-\mathbf{r}'-\lambda_{\alpha'}\xi'(s)|) \ . \quad (3.7)$$

This potential is different from the electrostatic interaction energy between two uniformly charged filaments, because the average of v_c is taken only over pairs of positions ξ and ξ' that correspond to the same s rather than over all pairs. However, it reduces to the Coulomb potential at large distances, i.e.,

$$v(\mathcal{E},\mathcal{E}')\sim 1/|\mathbf{r}-\mathbf{r}'| \quad \text{when } |\mathbf{r}-\mathbf{r}'|\to\infty \quad (3.8)$$

since the filaments can then be replaced by points.

The insertion of the FK representation (3.6) in the space-configurational expression (2.8) of $\Xi_\Lambda^{\mathrm{MB}}$ leads to a sum over the states of $\mathcal{S}^*$ weighted by Boltzmann factors for the filaments interactions. In this sum, it is quite natural to define the phase-space measure $d\mathcal{E}$ for a filament such that $d\mathcal{E}=d\alpha\, d\mathbf{r}\mathcal{D}(\xi)$ and to set $z(\mathcal{E})=(2\sigma_\alpha+1)z_\alpha/(2\pi\lambda_\alpha^2)^{3/2}$ for its fugacity. The above sum is then identified as the grand-partition function Ξ_Λ^* of $\mathcal{S}^*$, i.e.,

$$\Xi_\Lambda^{\mathrm{MB}}=\Xi_\Lambda^*=\sum_{N=0}^{\infty}\frac{1}{N!}\int\prod_{k=1}^{N} d\mathcal{E}_k z(\mathcal{E}_k)\prod_{\substack{k,l\\ k<l}}[1+f(\mathcal{E}_k,\mathcal{E}_l)] , \quad (3.9)$$

where $f(\mathcal{E}_k,\mathcal{E}_l)$ is the Mayer bond corresponding to $v(\mathcal{E}_k,\mathcal{E}_l)$, namely,

$$f(\mathcal{E}_k,\mathcal{E}_l)=\exp[-\beta e_{\alpha_k} e_{\alpha_l} v(\mathcal{E}_k,\mathcal{E}_l)]-1 \ . \quad (3.10)$$

The identity (3.9) exemplifies the equivalence between the quantum system $\mathcal{S}^{\mathrm{MB}}$ and the classical system $\mathcal{S}^*$ for studying equilibrium properties. In $\mathcal{S}^*$, the quantum-mechanical aspect of $\mathcal{S}^{\mathrm{MB}}$ is hidden in the complex nature of the filaments. In fact, these extended objects describe the quantum fluctuations of the point particles. In the effective-potential method [27], the auxiliary classical system is still made of point objects while the quantum effects are taken into account in the two-body and higher-order effective interactions. Here we stress that the interactions between the filaments are strictly of the two-body type.

C. Mayer-like expansions

The grand-partition function Ξ_Λ^* of $\mathcal{S}^*$ has the same mathematical structure as that of an ordinary one-

component classical system made of point particles interacting via two-body forces. Thus the thermodynamic correlation functions of S^* can be represented by Mayer-like diagrammatic expansions in either the fugacity $z(\mathcal{E})$ or the density $\rho(\mathcal{E})$. The corresponding graphs are built with f bonds which connect filaments instead of points. Their topological structure and symmetry-counting factors are defined via the usual classical rules [28]. The class of z graphs can be transformed into the class of ρ graphs by applying the familiar principle of topological reduction [28] based on the identity

$$\rho(\mathcal{E})=\lim_{\mathrm{TL}} z(\mathcal{E})\frac{\delta \ln \Xi_\Lambda^*}{\delta z(\mathcal{E})} . \tag{3.11}$$

This principle essentially amounts to suppressing the articulation points (filaments) defined in the following and which appear in the genuine class of z graphs. For instance, if we consider the two-point Ursell function [28] such that

$$\rho(\mathcal{E}_a)\rho(\mathcal{E}_b)h(\mathcal{E}_a,\mathcal{E}_b)=z(\mathcal{E}_a)z(\mathcal{E}_b)\lim_{\mathrm{TL}}\frac{\delta^2 \ln \Xi_\Lambda^*}{\delta z(\mathcal{E}_a)\delta z(\mathcal{E}_b)} \tag{3.12}$$

its Mayer density expansion reads

$$h(\mathcal{E}_a,\mathcal{E}_b)=\sum_\Gamma \frac{1}{S_\Gamma}\int \prod_{n=1}^{N} d\mathcal{E}_n \rho(\mathcal{E}_n)\left[\prod f\right]_\Gamma . \tag{3.13}$$

In (3.13), the sum runs over all the unlabeled topologically different and connected diagrams Γ's with two root filaments a,b and N internal filaments ($N=0,\ldots,\infty$), every filament having a unit weight. Moreover, a Γ diagram contains no articulation filament (such a filament is defined by the property that, if it is taken out of the diagram, then the latter is split into several pieces, at least one of which is no longer linked to any root filament). Each pair of filaments is linked by at most one f bond. $[\prod f]_\Gamma$ is the product of the f bonds in the Γ diagram and S_Γ is its symmetry factor, i.e., the number of permutations of the internal filaments $\mathcal{E}_n$ which do not change this product. For brevity, we have used the convention that if N is equal to 0, no $\int d\mathcal{E}_n\rho(\mathcal{E}_n)$ appears, and $[\prod f]_\Gamma$ reduces to $f(\mathcal{E}_a,\mathcal{E}_b)$. In Fig. 1, we have drawn a typical diagram which contributes to the right-hand side of (3.13).

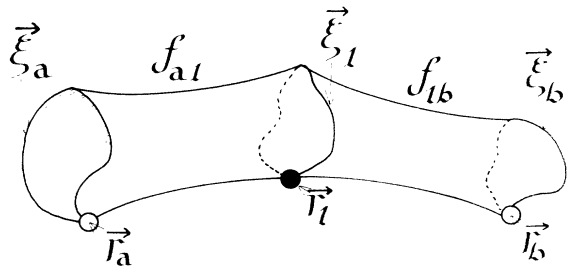

FIG. 1. A typical Mayer graph in the density expansion (3.13) of $h(\mathcal{E}_a,\mathcal{E}_b)$. The open circles are the positions of the root filaments $\mathcal{E}_a$ and $\mathcal{E}_b$, while the black circle denotes the position of the field filament $\mathcal{E}_l$. The closed curves starting from and ending at each of these positions represent the shapes of the corresponding filaments. The tubes connecting these curves are Mayer bonds.

The Mayer-like expansions of the MB quantities follow directly from the equivalence relation between $\mathcal{S}^{\mathrm{MB}}$ and $\mathcal{S}^*$. In particular, the diagrammatic expansion of the two-point truncated distribution function $\rho_T^{\mathrm{MB}}(\alpha_a\mathbf{r}_a,\alpha_b\mathbf{r}_b)$ is readily obtained through the functional integration of each graph in (3.13) over the shapes ξ_a and ξ_b of the root filaments $\mathcal{E}_a$ and $\mathcal{E}_b$ according to the equivalence identity

$$\rho_T^{\mathrm{MB}}(\alpha_a\mathbf{r}_a,\alpha_b\mathbf{r}_b)=\int \mathcal{D}(\xi_a)\mathcal{D}(\xi_b)\rho(\xi_a)\rho(\xi_b)h(\mathcal{E}_a,\mathcal{E}_b) . \tag{3.14}$$

Because of the long-range Coulombic nature of the filament potential v displayed through the behavior (3.8), all the above Mayer graphs diverge. In Sec. IV, we will show how these divergencies are eliminated by summing the contributions of an infinite number of graphs. In this procedure, we will take crucial advantage of the two-body bond structure of the Mayer graphs in the Feynman-Kac representation. In the genuine configuration representation, the density expansions cannot be written in terms of graphs built with only two-body bonds. This us due to the noncommutativity between the kinetic and the potential operators in the Hamiltonian $H_{N,\Lambda}$ which prevents expressing a space matrix element of $\exp(-\beta H_{N,\Lambda})$ as a product of two-body terms depending only on the relative positions of the particles. As far as formal infinite resummations are concerned, this difficulty intrinsic to quantum mechanics is circumvented by use of the Feynman-Kac representation [29]. However, for practical calculations, the difficulty relies on the functional integration over the shapes of the filaments. In particular, we stress that the filament density $\rho(\mathcal{E})$ depends on the shape of the filaments considered. Precise knowledge of this complicated shape dependence is not needed for performing the resummations described in Sec. IV. The method for calculating this functional in terms of the particle densities will be revealed in Sec. V.

IV. RESUMMATIONS OF THE LONG-RANGE COULOMB DIVERGENCIES

As in the classical case, it is particularly convenient to carry out the resummation procedure for the two-point Ursell function $h(\mathcal{E}_a,\mathcal{E}_b)$. The corresponding resummed diagrammatic expansions of the thermodynamic quantities can then be inferred via standard identities, to be given in the second paper of this series. For brevity, a filament in state $\mathcal{E}$ will be called a point $\mathcal{E}$, and it will be represented by a point in the figures. Moreover, we will omit the superscript MB, keeping in mind that all the quantities of $\mathcal{S}$ are calculated in the framework of Maxwell-Boltzmann statistics in the paper.

A. Topological structure of the chain resummation

We start with the Mayer expansion (3.13) of $h(\mathcal{E}_a,\mathcal{E}_b)$ in terms of the Γ diagrams built with the f bonds (3.10). We define $f_{\mathrm{as}}(\mathcal{E}_i,\mathcal{E}_j)$ as the asymptotic behavior of $f(\mathcal{E}_i,\mathcal{E}_j)$ at large distances up to the order

$O(1/r_{ij}^2)$ ($r_{ij}=|\mathbf{r}_i-\mathbf{r}_j|$). According to (3.10), if we use the notation $\beta_{ij}\equiv e_{\alpha_i}e_{\alpha_j}\beta$, then

$$f_{\rm as}(\mathcal{E}_i,\mathcal{E}_j)=-\beta_{ij}v_c(r_{ij}) -\beta_{ij}\int_0^1 ds[\lambda_{\alpha_i}\xi_i(s)\cdot\nabla_{\mathbf{r}_i} +\lambda_{\alpha_j}\xi_j(s)\cdot\nabla_{\mathbf{r}_j}]v_c(r_{ij}) +\frac{\beta_{ij}^2}{2}[v_c(r_{ij})]^2 . \quad (4.1)$$

In order to resum the divergencies induced by the nonintegrable part $f_{\rm as}$, we introduce the truncated f_T bond defined as

$$f_T\equiv f-f_{\rm as} \quad (4.2)$$

along with the f_C bond and the $\xi_i\cdot\nabla_i f_C$ bond defined as

$$f_C(\mathcal{E}_i,\mathcal{E}_j)\equiv-\beta_{ij}v_C(r_{ij}) \quad (4.3)$$

and

$$\lambda_{\alpha_i}\xi_i\cdot\nabla_i f_C(\mathcal{E}_i,\mathcal{E}_j)\equiv-\beta_{ij}\int_0^1 ds\,\lambda_{\alpha_i}\xi_i(s)\cdot\nabla_{\mathbf{r}_i}v_C(r_{ij}) . \quad (4.4)$$

With these definitions the f bond reads

$$f=f_T+f_C+\lambda_{\alpha_i}\xi_i\cdot\nabla_i f_C+\lambda_{\alpha j}\xi_j\cdot\nabla_j f_C+\frac{f_C^2}{2} . \quad (4.5)$$

Then $h(\mathcal{E}_a,\mathcal{E}_b)$ can be expressed by the same formula as (3.13) where now the Γ diagrams are replaced by $\tilde{\Gamma}$ diagrams made with $\tilde{f}$ bonds which are equal either to f_T, f_C, $\lambda_{\alpha_i}\xi_i\cdot\nabla_i f_C$, or $f_C^2/2$. The Γ and $\tilde{\Gamma}$ diagrams have the same topological properties.

We are interested in summing the contributions from all the "Coulomb chains" defined as follows. A "plain Coulomb chain" between the points $\mathcal{E}_i$ and $\mathcal{E}_j$ is a convolution chain of f_C bonds between these two points and an "i-derived (j-derived) Coulomb chain" is a convolution where the bond linked to $\mathcal{E}_i$ ($\mathcal{E}_j$) is $\lambda_{\alpha_i}\xi_i\cdot\nabla_i f_C$ ($\lambda_{\alpha j}\xi_j\cdot\nabla_j f_C$) and the other bonds in the chain are f_C bonds. These convolutions may either reduce to a single bond or contain intermediate points. Moreover there are i- and j-derived Coulomb chains where the bond linked to $\mathcal{E}_i$ is $\lambda_{\alpha_i}\xi_i\cdot\nabla_i f_C$, that linked to $\mathcal{E}_j$ is $\lambda_{\alpha j}\xi_j\cdot\nabla_j f_C$, and there are possible f_C bonds between them. The intermediate points of the convolutions $f_C\circ f_C$, $[\lambda_{\alpha_i}\xi_i\cdot\nabla_i f_C]\circ f_C$, $f_C\circ[\lambda_{\alpha j}\xi_j\cdot\nabla_j f_C]$, or $[\lambda_{\alpha_i}\xi_i\cdot\nabla_i f_C]\circ[\lambda_{\alpha j}\xi_j\cdot\nabla_j f_C]$ are called "Coulomb points" in the following. We notice that we can make a partition of the $\tilde{\Gamma}$ diagrams such that every diagram in a given class leads to the same so-called prototype Π diagram when all the Coulomb points are integrated over. In Figs. 2(a)–2(c), we show three $\tilde{\Gamma}$ diagrams belonging to the same resummation class. The points $\mathcal{P}_i$ which are left over in the chain resummation are still linked in the Π diagram by two-body bonds $F(\mathcal{P}_i,\mathcal{P}_j)$. There are four kinds of F bonds and we call F a "plain" F bond if $\mathcal{P}_i$ and $\mathcal{P}_j$ were linked in the $\tilde{\Gamma}$ diagram by a single plain Coulomb chain, an i- (j-) derived F bond if they were linked in the $\tilde{\Gamma}$ diagram by a single i- (j-) derived Coulomb chain, an i- and j-derived F bond if they were linked in the $\tilde{\Gamma}$ diagram by a single i- and j-derived Coulomb chain [30], and a "dressed" F bond in other cases.

The above procedure for defining the Π diagrams implies that between two points $\mathcal{P}_i$ and $\mathcal{P}_j$ of any diagram Π there cannot appear a convolution of two plain F bonds, a convolution of an i-derived F bond and a plain F

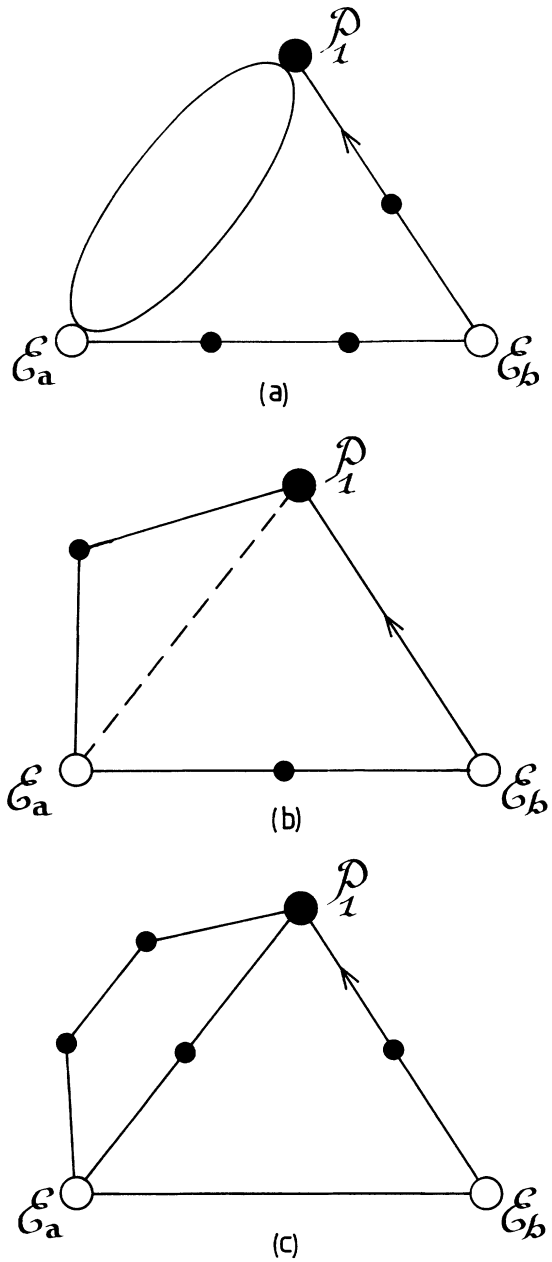

FIG. 2. Three $\tilde{\Gamma}$ diagrams contributing to $h(\mathcal{E}_a,\mathcal{E}_b)$. The open circles represent the root points. The big black circle is the field point which is left over in the resummation process. The small black circles are Coulomb points. The bonds f_C, $f_C^2/2$, $\lambda_{\alpha_i}\xi_i\cdot\nabla_i f_C$, and f_T are, respectively, represented by single straight lines, double curved lines, single straight lines with an arrow, and single dashed lines (the direction of the arrow indicates the i point in $\lambda_{\alpha_i}\xi_i\cdot\nabla_i f_C$).

bond ending at $\mathcal{P}_j$, a convolution of a plain F bond starting at $\mathcal{P}_i$ and a j-derived F bond, or a convolution of an i-derived F bond and a j-derived F bond. If we keep the above four kinds of bonds together with the latter topological rules for building the Π diagrams, the sum of the $\tilde{\Gamma}$ diagrams exactly reduces to a sum of Π diagrams, i.e.,

$$h(\mathcal{C}_a,\mathcal{C}_b)=\sum_{\tilde{\Gamma}}\frac{1}{S_{\tilde{\Gamma}}}\int\prod_{n=1}^{N}d\mathcal{C}_n\rho(\mathcal{C}_n)\left[\prod\tilde{f}\right]_{\tilde{\Gamma}}$$
$$=\sum_{\Pi}\frac{1}{S_{\Pi}}\int\prod_{m=1}^{M}d\mathcal{P}_m\rho(\mathcal{P}_m)\left[\prod F\right]_{\Pi}, \tag{4.6}$$

as shown in the Appendix. The resummed F bonds take the form

$$F(\mathcal{P}_i,\mathcal{P}_j)=\sum_{\tilde{\Gamma}_{ij}}\frac{1}{S_{\tilde{\Gamma}_{ij}}}\int\prod_{k=1}^{n_{ij}}d\mathcal{C}_k^{\{ij\}}\rho(\mathcal{C}_k^{\{ij\}})\left[\prod\tilde{f}\right]_{\tilde{\Gamma}_{ij}}, \tag{4.7}$$

where the sum runs over all the unlabeled $\tilde{\Gamma}_{ij}$ diagrams which are built between the two root points $\mathcal{P}_i$ and $\mathcal{P}_j$ by adding Coulomb chains made with $n_{ij}\mathcal{C}_k^{\{ij\}}$ Coulomb points according to the prescriptions described above. We notice that the expression (4.7) for a bond $F(\mathcal{P}_i,\mathcal{P}_j)$ between a given pair $\{ij\}$ does not depend on the global structure of the considered prototype diagram. In other words, the simultaneous resummations of the Coulomb chains between the various pairs $\{ij\}$ are completely decoupled. We stress that the topological structure of the Mayer Γ diagrams is conserved through the resummation process, with, in addition, the above excluded-convolution rule which avoids double counting.

B. Calculation of the resummed bonds

Let us first compute the plain F bond. Since the f_C bonds are shape independent, the functional integrations over the shapes of the intermediate $\mathcal{C}_k^{\{ij\}}$ filaments lead to the replacement of $\rho(\mathcal{C}_k^{\{ij\}})$ by the particle density ρ_{α_k}. Thus the summation of all the present convolution chains can be performed in terms of the familiar Debye potential $\phi_D(r)=\exp(-\kappa r)/r$ [with $\kappa=(4\pi\beta\sum_\alpha e_\alpha^2\rho_\alpha)^{1/2}$], and the plain F bond is merely equal to

$$f_D(\mathcal{P}_i,\mathcal{P}_j)\equiv-\beta_{ij}\phi_D(r_{ij}). \tag{4.8}$$

In the same way the i-derived F bond, which is the sum of all the single Coulomb chains which are linked to the point $\mathcal{P}_i$ by a $\lambda_{\alpha_i}\xi_i\cdot\nabla_i f_C$ bond, is equal to $\lambda_{\alpha_i}\xi_i\cdot\nabla_i f_D$ with

$$\lambda_{\alpha_i}\xi_i\cdot\nabla_i f_D(\mathcal{P}_i,\mathcal{P}_j)\equiv-\beta_{ij}\int_0^1 ds\,\lambda_{\alpha_i}\xi_i(s)\cdot\nabla_{\mathbf{r}_i}\phi_D(r_{ij}) \tag{4.9}$$

whereas the i and j-derived F bond reads

$$f_{\rm dip}(\mathcal{P}_i,\mathcal{P}_j)\equiv-\beta_{ij}\int_0^1 ds\int_0^1 ds'[\lambda_{\alpha_i}\xi_i(s)\cdot\nabla_{\mathbf{r}_i}]\times[\lambda_{\alpha_j}\xi_j(s')\cdot\nabla_{\mathbf{r}_j}]\times[\phi_D-v_c](r_{ij}). \tag{4.10}$$

At large distances, the $f_{\rm dip}$ bond behaves as the dipole-dipole electrostatic potential between the filaments $\mathcal{P}_i$ and $\mathcal{P}_j$.

Now we turn to the dressed F bond which involves the other basic bonds f_T and $f_C^2/2$ and products of Coulomb chains. In the $\tilde{\Gamma}$ diagrams each pair of points is linked by at most one basic bond f_T, f_C, $\frac{1}{2}f_C^2$, $\lambda_{\alpha_i}\cdot\xi_i\nabla_i f_C$, or $\lambda_{\alpha j}\cdot\xi_j\nabla_j f_C$. So when one or several Coulomb chains are multiplied by a basic bond, these Coulomb chains must be genuine chains, i.e., chains which contain at least one internal point. Then it is convenient to compute the dressed F bond as the sum of the contributions from (a) either the basic f_T bond or the basic $f_C^2/2$ bond; (b) one of the basic bonds f_T, f_C, $f_C^2/2$, $\lambda_{\alpha_i}\xi_i\cdot\nabla_i f_C$, or $\lambda_{\alpha j}\xi_j\cdot\nabla_j f_C$ multiplied by a product of q, with $q\geq 1$, genuine Coulomb chains (which can be either plain, i derived, j derived, or i and j derived); and (c) a product of q, with $q\geq 2$, genuine Coulomb chains (which can be either plain, i derived, j derived, or i and j derived). Every case is illustrated in Figs. 2(a), 2(b), and 2(c), respectively, where the dressed bond connects $\mathcal{C}_a$ and $\mathcal{P}_1$.

We first calculate the contribution of the single genuine Coulomb chains. In these chains, as in the case of the plain or derived F bonds, the shape independence of the f_C bonds allows replacing $\rho(\mathcal{C}_k^{\{ij\}})$ by ρ_{α_k}, and the summation makes the Debye potential reappear. Then, the considered contribution is $-\beta_{ij}\psi_{ch}$ with

$$\psi_{ch}(\mathcal{P}_i,\mathcal{P}_j)=(\phi_D-v_C)(r_{ij})+[\lambda_{\alpha_i}\xi_i\cdot\nabla_i+\lambda_{\alpha_j}\xi_j\cdot\nabla_j](\phi_D-v_C)(r_{ij})+[\lambda_{\alpha_i}\xi_i\cdot\nabla_i]\cdot[\lambda_{\alpha_j}\xi_j\cdot\nabla_j](\phi_D-v_C)(r_{ij}), \tag{4.11}$$

where the substraction of the Coulomb potential is due to the absence of any direct bond connecting $\mathcal{P}_i$ and $\mathcal{P}_j$ in the genuine chains.

Now we turn to the contribution from the Γ_{ij} diagrams which are products of q genuine Coulomb chains between the two points $\mathcal{P}_i$ and $\mathcal{P}_j$. Let Δ be such a diagram. The general form of its contribution can be found by the following topological argument. After integration over the intermediate points $\mathcal{C}_k^{\{ij\}}$, $\int\prod_{k=1}^{n_{ij}}d\mathcal{C}_k^{\{ij\}}\rho(\mathcal{C}_k^{\{ij\}})[\prod\tilde{f}]_\Delta$ is just the product of the contributions from every chain. Moreover, the contribution of a given chain is a function $I(c)$ which depends only on the number c of intermediate points in the chain and the symmetry factor of the diagram is just $\prod_{c=1}^{\infty}q_c!$, where q_c is the number of chains in the diagram Δ which have c intermediate points. Thus the sum over all the topologically different diagrams made with q chains reads

$$\sum_{\{q_1,\ldots,q_\infty\}/\sum_{c=1}^{\infty}q_c=q}\prod_{c=1}^{\infty}\frac{1}{q_c!}\prod_{c=1}^{\infty}I(c)^{q_c}=\frac{1}{q!}\left[\sum_{c=1}^{\infty}I(c)\right]^q. \tag{4.12}$$

In the present case $\sum_{c=1}^{\infty}I(c)$ is equal to $-\beta_{ij}\psi_{ch}$ and the contribution from the products of q chains is $(-\beta_{ij}\psi_{ch})^q/q!$. Thus the dressed F bond is the sum of

the contributions

$$f_T+\tfrac{1}{2}f_C^2\ , \tag{4.13a}$$

$$f[e^{-\beta_{ij}\psi_{ch}}-1]\ , \tag{4.13b}$$

$$e^{-\beta_{ij}\psi_{ch}}-1+\beta_{ij}\psi_{ch}\ , \tag{4.13c}$$

which reads

$$\begin{aligned} f_R=&e^{-\beta_{ij}(v+\psi_{ch})}-1 \\ &+\beta_{ij}\{\phi_D+[\lambda_{\alpha_i}\xi_i\cdot\nabla_i+\lambda_{\alpha_j}\xi_j\cdot\nabla_j]\phi_D \\ &\quad+[\lambda_{\alpha_i}\xi_i\cdot\nabla_i][\lambda_{\alpha_j}\xi_j\cdot\nabla_j](\phi_D-v_C)\} \end{aligned} \tag{4.14}$$

after combining (3.10), (4.11), and (4.5). We notice that f_R depends on the density only through the inverse Debye-Hückel length κ.

According to the topological analysis of Sec. IV A, two points of the diagram Π are connected by at most one bond, either an f_D bond, a $\lambda_{\alpha_i}\xi_i\cdot\nabla_i f_D$ bond, an $f_{\rm dip}$ bond, or an f_R bond. Furthermore, the excluded-convolution rule stipulates that between two points $\mathcal{P}_i$ and $\mathcal{P}_j$ there cannot appear either a convolution $f_D\circ f_D$, $[\lambda_{\alpha_i}\xi_i\cdot\nabla_i f_D]\circ f_D$, $f_D\circ[\lambda_{\alpha j}\xi_j\cdot\nabla_j f_D]$, or $[\lambda_{\alpha_i}\xi_i\cdot\nabla_i f_D]\circ[\lambda_{\alpha j}\xi_j\cdot\nabla_j f_D]$. If we set $\lambda_{\alpha_i}=0$, the derived bonds disappear, f_R reduces to $\exp(-\beta_{ij}\phi_D)-1+\beta_{ij}\phi_D$, and we recover the Meeron classical result [10]. In Fig. 3, we draw the Π graph generated by the resummation of all the $\tilde{\Gamma}$ diagrams belonging to the same class as those shown in Fig. 2.

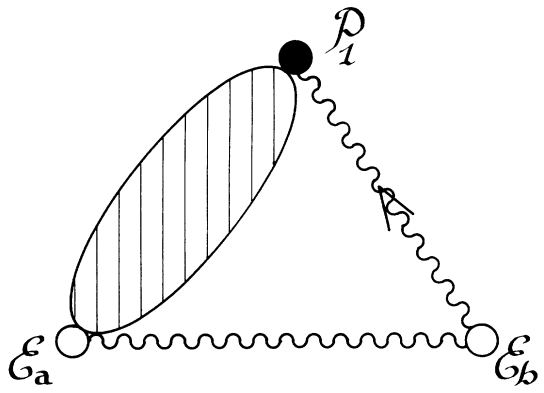

FIG. 3. The prototype Π graph generated by the resummation of all the $\tilde{\Gamma}$ diagrams belonging to the same class as those shown in Fig. 2. The hatched bubble represents and f_R bond. The wavy line, without and with an arrow, are bonds f_D and $\lambda_\alpha\xi\cdot\nabla f_D$, respectively (the direction of the arrow has the same meaning as in Fig. 2).

C. Integrability of the Π diagrams

At this level, it remains to show that the integrals over the internal points of any Π diagram are convergent. The functional integrations over the shapes of the filaments surely are well behaved because of the Gaussian decay of the measure $D(\xi)$ [it is quite reasonable to assume that the functional $\rho(\mathcal{P})$ does not explode faster than a Gaussian function for large filaments]. In the original Γ diagrams, the possible short-distance singularities of the Mayer bonds f are smoothed out by the functional integrations according to the Gaussian measure $\mathcal{D}(\xi)$ [31]. In the present Π diagrams, there may be spurious nonintegrable singularities at $\mathbf{r}=\mathbf{0}$ arising from the introduction of auxiliary $\tilde{f}$ bonds which diverge at the origin. In fact, these spurious divergencies already appear in the classical Abe-Meeron expansion as pointed out by Lavaud [32]. In principle, they should cancel out by suitably collecting together the dangerous graphs.

The long-range divergencies in the original Γ diagrams are expected to be eliminated by the resummation process. In fact, we will show below that the Π graphs are indeed integrable at large distances. Obviously, f_D and $\lambda_{\alpha_i}\xi_i\cdot\nabla_i f_D$ decay exponentially fast, but the study of the contributions of f_R and $f_{\rm dip}$ requires more care. According to the definition (3.10) of f, we can rewrite f_R as

$$\begin{aligned} f_R=&\exp\{-\beta_{ij}(v-v_C-[\lambda_{\alpha_i}\xi_i\cdot\nabla_i+\lambda_{\alpha_j}\xi_j\cdot\nabla_j]v_C-[\lambda_{\alpha_i}\xi_i\cdot\nabla_i][\lambda_{\alpha_j}\xi_j\cdot\nabla_j]v_C)\} \\ &\times\exp\{-\beta_{ij}(\phi_D+[\lambda_{\alpha_i}\xi_i\cdot\nabla_i+\lambda_{\alpha_j}\xi_j\cdot\nabla_j]\phi_D+[\lambda_{\alpha_i}\xi_i\cdot\nabla_i][\lambda_{\alpha_j}\xi_j\cdot\nabla_j]\phi_D)\} \\ &-1+\beta_{ij}\{\phi_D+[\lambda_{\alpha_i}\xi_i\cdot\nabla_i+\lambda_{\alpha_j}\xi_j\cdot\nabla_j]\phi_D+[\lambda_{\alpha_i}\xi_i\cdot\nabla_i][\lambda_{\alpha_j}\xi_j\cdot\nabla_j](\phi_D-v_c)\}\ . \end{aligned} \tag{4.15}$$

Since ϕ_D decays exponentially fast at large distances, the leading algebraic term in the asymptotic behavior of f_R is immediately obtained from (4.15) by setting $\phi_D=0$ and by replacing v by its multipolelike expansion. The monopole-monopole and dipole-monopole terms cancel out in the argument of the first exponential of (4.15). The first nonvanishing term comes from the dipole-dipole-like interactions and leads to

$$f_R\sim-\beta_{ij}\frac{1}{2!}\int_0^1 ds[\lambda_{\alpha_i}\xi_i(s)\cdot\nabla_i+\lambda_{\alpha_j}\xi_j(s)\cdot\nabla_j]^2 v_C(r_{ij})\ ,$$

$$r_{ij}\to\infty\ . \tag{4.16}$$

This shows that f_R decays only as $1/r^3$ at large distances, as f_T itself. From the definition (4.10), it is obvious that $f_{\rm dip}$ decays as $1/r^3$ also. Although this power law is at the border line for integrability, it does not cause any logarithmic divergency because the Π diagrams are sufficiently connected [33]. The integrability is indeed essentially ensured by the following simple mechanism. When a cluster of points is sent to infinity, the product of the bonds $[\prod F]_\Pi$ decays at least as $1/R^6$ because the absence of articulation points guarantees that this cluster is connected via at least two bonds to the remaining part of the diagram considered. Thus every Π diagram is inte-

grable at large distances as required.

The structure (4.8), (4.9), and (4.15) of the resummed bonds f_D, $\lambda_{\alpha_i}\xi_i\cdot\nabla_i f_D$, and f_R, respectively, show that the monopole-monopole and dipole-monopole interactions are exponentially screened as in the classical case. Moreover, it turns out that this screening mechanism is entirely controlled by the classical Debye length κ^{-1}. The higher-order multipole interactions should not be screened so efficiently, as indicated by the slow decays of f_R and $f_{\rm dip}$. This should ultimately induce algebraic tails in the correlations in agreement with the predictions of Refs. [20] and [21].

D. Diagrammatic expansion of $\rho_T^{\rm MB}(\alpha_a \mathbf{r}_a, \alpha_b \mathbf{r}_b)$

The required diagrammatic expansion of the two-point correlations of $\mathcal{S}^{\rm MB}$ is immediately obtained by inserting the Π diagram representation (4.6) in the identity (3.14). Each graph is multiplied by $\rho(\mathcal{E}_a)\rho(\mathcal{E}_b)$ and integrated over the shapes ξ_a and ξ_b of the root filaments $\mathcal{E}_a$ and $\mathcal{E}_b$.

Strictly speaking, the previous diagrammatic representation of $\rho_T^{\rm MB}(\alpha_a \mathbf{r}_a, \alpha_b \mathbf{r}_b)$ does not constitute an explicit expansion with respect to the particle densities ρ_α, in the sense that the statistical weights of the points in the graphs are the shape-dependent filament densities. In fact, the functional $\rho(\mathcal{E})$ can be itself expanded in powers of the particle densities as shown in Sec. V.

V. THE FUNCTIONAL $\rho(\mathcal{E})$

In this section we show how the functional $\rho(\mathcal{E})$ can be calculated from the particle densities ρ_γ. We start from the Mayer-like expansion of $\rho(\mathcal{E})$ in powers of the filament fugacities, $z(\mathcal{E})=(2\sigma_\alpha+1)z_\alpha/(2\pi\lambda_\alpha^2)^{3/2}$, which do not depend on the shapes of the filaments [for notational convenience, we set $z(\mathcal{E})=z_\alpha^*$ in the following]. In Sec. V A, we give the topological prescriptions which define the corresponding Mayer z graphs. The familiar degenerescence in the fugacities, which is induced by the neutrality condition (2.5) specific to Coulomb systems, is also discussed and exploited. The long-range Coulomb divergencies are resummed in Sec. V B. This provides a diagrammatic representation of $\rho(\mathcal{E})$ in terms of prototype graphs built with resummed bonds partly scaled by $\kappa_z=(4\pi\beta\sum_\alpha e_\alpha^2 z_\alpha^*)^{1/2}$ instead of κ. In Sec. V C, we produce simple arguments showing that these resummed prototype graphs do converge. We show that each prototype graph can be expanded in a double integer series with respect to $z^{1/2}$ and $\ln z$ in Sec. V D. In Sec. V E, the structure of the corresponding fugacity expansion of $\rho(\mathcal{E})$ is derived and the first two terms of it are computed. The required particle-density expansion of $\rho(\mathcal{E})$ is then inferred and calculated explicitly up to order ρ^2, in Sec. V F.

A. Grand-canonical representation of $\rho(\mathcal{E})$

In the framework of the grand-canonical ensemble, the functional $\rho(\mathcal{E})$ depends on the fugacities z_γ^* and on the temperature, of course. Once the thermodynamic limit has been taken, the functional $\rho(\mathcal{E})$ becomes translationally invariant, i.e., $\rho(\mathcal{E})=\rho_\alpha(\xi)$, while the particle densities $\rho_\alpha=\int\mathcal{D}(\xi)\rho_\alpha(\xi)$ satisfy the neutrality condition (2.5) for any set of fugacities [18]. The possible excess charges always go to the boundaries, where they form an electrical double layer, the total surface charge of which is controlled by a specific combination of the fugacities [23]. Since the n_s bulk densities involve only (n_s-1) independent functions of the n_s fugacities, a continuous family of sets $\{z_\gamma^*\}$ belonging to a one-dimensional curve in the n_s-dimensional fugacity space is associated with each set $\{\rho_\alpha\}$ of the particle densities satisfying (2.5).

In principle, the above degenerescence is automatically taken into account in the fugacity expansion of $\rho_\alpha(\xi)$. However, in the following, for reasons of technical convenience, we split this degenerescence by adding the constraint

$$\sum_\alpha e_\alpha z_\alpha^* = 0 \ . \tag{5.1}$$

This specifies a bijective relation between the ρ's and the z^*'s (at a given temperature). In the n_s-dimensional fugacity space, the unique point $\{z_\gamma^*\}$ corresponding now to a given set $\{\rho_\alpha\}$ is the intersection of the above degenerescence curve with the hyperplane defined by (5.1). The arbitrary constraint (5.1) is also the most natural, since it guarantees that ρ_α behaves as z_α^* in the small-fugacity limit, as shown later.

The fugacity Mayer expansion of the density $\rho_\alpha(\xi)$ reads in a way similar to that of $h(\mathcal{E}_a,\mathcal{E}_b)$

$$\rho_\alpha(\xi)=z_\alpha^*\sum_G\frac{1}{S_G}\int\prod_{n=1}^{N}d\mathcal{E}_n z_{\alpha_n}^*\left[\prod f\right]_G \ , \tag{5.2}$$

where the definitions are the same as in (3.13) apart from the following topological differences: the connected G diagrams have only one root point $\mathcal{E}$ and they may contain articulation points. Moreover, the weight $\rho(\mathcal{E}_n)$, which appears in (3.13), is replaced by $z_{\alpha_n}^*$ in (5.2). All the above Mayer graphs diverge, like those defining $h(\mathcal{E}_a,\mathcal{E}_b)$ in (3.13), because of the long-range Coulomb nature of the filament potential v. These long-range divergencies will be again formally resummed in the infinite volume.

B. The resummed fugacity expansion of $\rho_\alpha(\xi)$

The scheme for the resummation of the long-range Coulomb divergencies is the same as that used in Sec. IV A with the decomposition (4.5) and the introduction of prototype P diagrams along with the analog of the previous excluded-convolution rule. However, the existence of articulation points in the $\tilde{G}$ diagrams implies not only that the P diagrams may contain articulation points too, but also that there exist rings which disappear when the Coulomb points are integrated over: these are the convolution rings where all the intermediate points are Coulomb ones and are not connected to any point outside the ring. As a consequence the weight of the $\mathcal{P}_m$ points which are left over in the resummation process is changed from $z_{\alpha_m}^*$ to $W(\mathcal{P}_m)$ which depends on the role

of $\mathcal{P}_m$ in the topology of the P diagram; in the meantime, the exclusion rules are reexpressed in order to take weight into account.

The reason for the existence of resummed bonds and weights, generic for all the diagrams, is similar to that explained in Appendix A for the resummation of the $\tilde{\Gamma}$ graphs. For each labeled diagram $\tilde{G}_{\rm lab}$, $[\Pi\tilde{f}]_{\tilde{G}_{\rm lab}}$ can be factored as

$$\prod_{\text{pairs}\{ij\}} \left[\Pi\tilde{f}\right]_{\tilde{G}_{ij}} \prod_i \left[\Pi f_C\right]_{\tilde{G}_{Ai}} ,$$

where $\tilde{G}_{ij}$ is the part of $\tilde{G}_{\rm lab}$ which connects $\mathcal{P}_i$ to $\mathcal{P}_j$ directly and/or by products of Coulomb chains and $\tilde{G}_{Ai}$ is the part of $\tilde{G}_{\rm lab}$ which is made of plain, i-derived, or twice i-derived Coulomb rings which are directly attached to $\mathcal{P}_i$ ($\mathcal{P}_i$ being their common articulation point). When we first integrate over the Coulomb points we have to choose the labels for the M $\mathcal{P}_i$'s, for the n_{ij} Coulomb points of every $\tilde{G}_{ij}$, and for the n_{Ai} Coulomb points in the Coulomb rings which are attached to every $\mathcal{P}_i$. The number of ways of choosing these labels is $N!/(M!\prod_{\{i,j\}} n_{ij}!\prod_i n_{Ai}!)$. So the analog of (4.6) reads

$$\rho_\alpha(\xi)=z^*_\alpha \sum_{\tilde{G}} \frac{1}{S_{\tilde{G}}} \int \prod_{n=1}^{N} d\mathcal{E}_n z^*_{\alpha_n} \left[\Pi\tilde{f}\right]_{\tilde{G}}$$
$$=\sum_P \frac{1}{S_P} W(\mathcal{E}_a) \int \prod_{m=1}^{M} d\mathcal{P}_m W(\mathcal{P}_m) \left[\Pi F_z\right]_P . \tag{5.3}$$

The expression for $F_z(\mathcal{P}_i,\mathcal{P}_j)$ depends on $\kappa_z=(4\pi\beta\sum_\alpha e^2_\alpha z^*_\alpha)^{1/2}$ instead of $\kappa=(4\pi\beta\sum_\alpha e^2_\alpha \rho_\alpha)^{1/2}$ since the summations involve points with a weight $z^*_{\alpha_n}$ instead of $\rho(\mathcal{E}_n)$.

In order to avoid counting some rings twice, we introduce P diagrams made with two kinds of points: "bare" points and "dressed" points. A bare point is a point which has no Coulomb rings attached to it in the $\tilde{G}$ diagrams which lead to the diagram P by the summation scheme, whereas a dressed point has at least one ring attached to it in the $\tilde{G}$ diagrams. Hence the weight of a bare point $\mathcal{P}_m$ is $z^*_{\alpha_m}$ whereas that of a dressed point is $W_r(\mathcal{P}_m)$, where $W_r(\mathcal{P}_m)$ is the sum of the contributions from all the Coulomb rings which may be attached directly to the point $\mathcal{P}_m$ in the $\tilde{G}$ diagrams. Three $\tilde{G}$ diagrams which belong to the same resummation class are drawn in Figs. 4(a)–4(c).

According to the same topological argument as that used in Sec. IV B, $W_r(\mathcal{P}_m)$ can be expressed in terms of an exponential

$$W_r(\mathcal{P}_m)=z^*_{\alpha_m}[e^{I_r(\mathcal{P}_m)}-1] , \tag{5.4}$$

where I_r is the sum of the plain, i-derived, or twice i-derived rings of all the possible lengths attached alone to the point $\mathcal{P}_m$. The contribution of the plain rings reads

$$-\frac{1}{2}\beta e^2_{\alpha_m}[\phi_{Dz}-v_C](r=0)=\frac{\beta}{2}e^2_{\alpha_m}\kappa_z , \tag{5.5}$$

where $\frac{1}{2}$ is the symmetry factor of a plain ring diagram and the substraction of v_c reflects the fact that a ring of f_C bonds contains at least one internal point. The sum of the i-derived rings (which contain at least two Coulomb points) is

$$\beta^2 e^2_{\alpha_m}\lambda_{\alpha_m}\sum_\alpha z^*_\alpha e^2_\alpha \int d\mathbf{r}\, v_c(\mathbf{r}-\mathbf{r}_m)$$
$$\times\int_0^1 ds\, \xi_m(s)\cdot\nabla_{\mathbf{r}_m}[\phi_{Dz}-v_C](\mathbf{r}-\mathbf{r}_m)=0 . \tag{5.6}$$

It vanishes because of the rotational invariance of the potentials ϕ_{Dz} and v_C, whereas the twice i-derived rings lead to

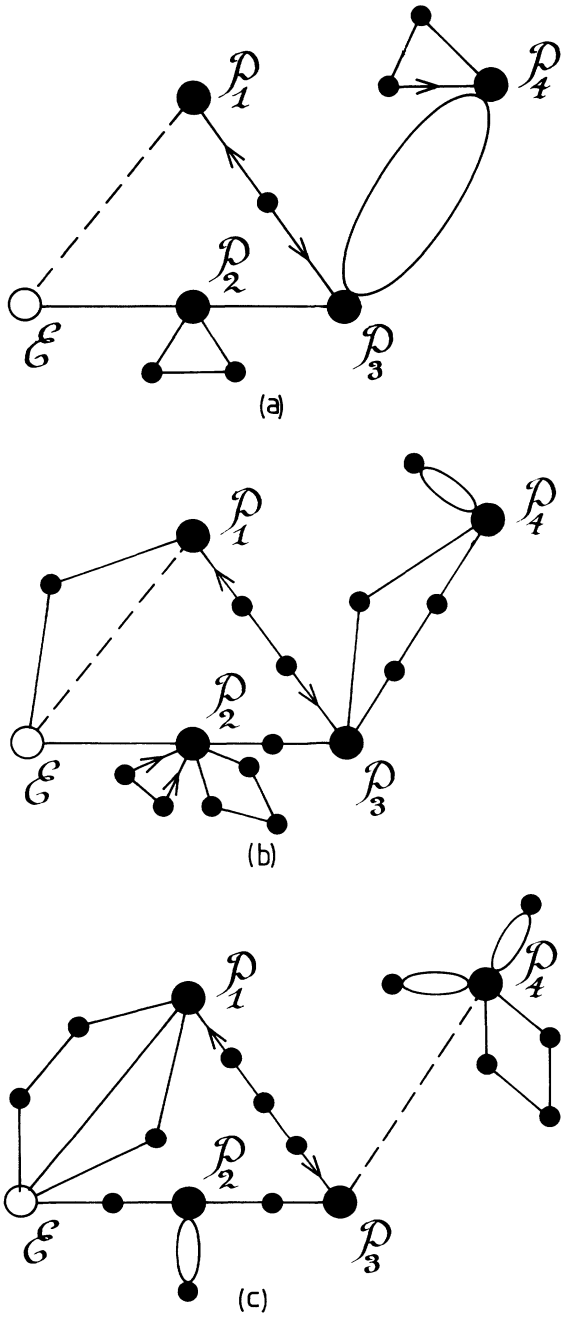

FIG. 4. Three $\tilde{G}$ diagrams contributing to $\rho(\mathcal{E})$.

$$\tfrac{1}{2}\beta^2 e_{\alpha_m}^2 \lambda_{\alpha_m}^2 \sum_\alpha z_\alpha^* e_\alpha^2 \int d\mathbf{r} \int_0^1 ds\, \xi_m(s)\cdot\nabla_{\mathbf{r}_m} v_C(\mathbf{r}-\mathbf{r}_m) \times \int_0^1 ds' \xi_m(s')\cdot\nabla_{\mathbf{r}_m}[\phi_{Dz}-v_C](\mathbf{r}-\mathbf{r}_m) = -\tfrac{1}{6}\beta e_{\alpha_m}^2 \lambda_{\alpha_m}^2 \kappa_z^3 \sum_\mu \left[\int_0^1 ds[\xi_m(s)]_\mu\right]^2 . \quad (5.7)$$

Eventually $I_r(\mathcal{P}_m)$ reads

$$I_r(\mathcal{P}_m)=\tfrac{1}{2}\beta e_{\alpha_m}^2 \kappa_z - \tfrac{1}{6}\beta e_{\alpha_m}^2 \lambda_{\alpha_m}^2 \kappa_z^3 \sum_\mu \left[\int_0^1 ds[\xi_m(s)]_\mu\right]^2 . \quad (5.8)$$

Contrarily to the bare weight $z_{\alpha_m}^*$, the dressed weight $W_r(\mathcal{P}_m)$ depends on the shape $\xi_m(s)$ of the filament $\mathcal{P}_m$.

Now we turn to the explicit value of the bonds. The summation involves weights $z_{\alpha_n}^*$ instead of $\rho(\mathcal{E}_n)$, so the bonds f_D, $\lambda_{\alpha_i}\xi_i\cdot\nabla_i f_D$, and f_{dip} are replaced by bonds f_{Dz}, $\lambda_{\alpha_i}\xi_i\cdot\nabla_i f_{Dz}$, and f_{dipz}, respectively, with κ_z in place of κ. In the same way the value of the generic dressed bond f_{Rz} is the same as that of Sec. IV with ρ_α changed into z_α^*. However, the dressed bond between an articulation point $\mathcal{P}_i$ and a point $\mathcal{P}_j$ which is not connected to any other point must be handled with care in order not to count any ring twice. If $\mathcal{P}_j$ is a dressed point [with a weight $W_r(\mathcal{P}_j)$] the dressed bond is the generic one f_{Rz}, but, if $\mathcal{P}_j$ is a bare point, the dressed bond is reduced to f_{Rz} minus the contributions where $\mathcal{P}_j$ would be in fact a Coulomb point in a ring attached to $\mathcal{P}_i$. The corresponding truncated dressed bond is

$$f_{Rz}^T(\mathcal{P}_i,\mathcal{P}_j)=f_{Rz}-\tfrac{1}{2}f_{Dz}^2 -[f_{Dz}\lambda_{\alpha_i}\xi_i\cdot\nabla_i f_{Dz}-f_C\lambda_{\alpha_i}\xi_i\cdot\nabla_i f_C] -\tfrac{1}{2}[(\lambda_{\alpha_i}\xi_i\cdot\nabla_i f_{Dz})^2-(\lambda_{\alpha_i}\xi_i\cdot\nabla_i f_C)^2] , \quad (5.9)$$

where the substractions of $f_C\lambda_{\alpha_i}\xi_i\cdot\nabla_i f_C$ and $(\lambda_{\alpha_i}\xi_i\cdot\nabla_i f_C)^2$ reflect the fact that any two points in the $\tilde{G}$ diagrams are linked by at most one basic bond.

We notice that, contrarily to the Π diagrams involved in the $\rho(\mathcal{E})$ expansion of $h(\mathcal{E}_a,\mathcal{E}_b)$, the P diagrams are built with five resummed bonds instead of four. The present extra bond f_{Rz}^T decays as $1/r^3$ at large distances. As in the case of the Π diagrams, there is at most one resummed bond between two points. In particular, there exists no ring made with only one intermediate point (such rings are already resummed in the expression of the dressed bond). Moreover, the excluded-convolution rule implied by the summation scheme still exists: the midpoint $\mathcal{P}_m$ of a chain made either with two f_{Dz} bonds, with a f_{Dz} bond and a $\lambda_{\alpha_i}\xi_i\cdot\nabla_i f_{Dz}$ bond (with $i\neq m$), or with a $\lambda_{\alpha_i}\xi_i\cdot\nabla_i f_{Dz}$ bond and a $\lambda_{\alpha_j}\xi_j\cdot\nabla_j f_{Dz}$ bond (with $i\neq m$ and $j\neq m$) must be a dressed point. In Fig. 5, we show the P graph generated by the resummation of all the $\tilde{G}$ diagrams belonging to the same class as those shown in Fig. 4.

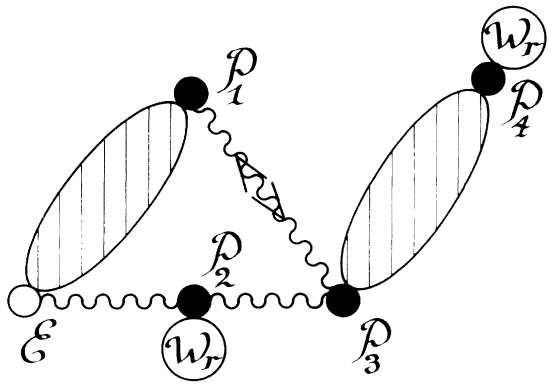

FIG. 5. The P graph generated by the resummation of all the $\tilde{G}$ diagrams belonging to the same class as those shown in Fig. 4. The hatched bubbles and the wavy lines represent bonds f_{Rz} and f_{Dz}, respectively, while the wavy line with two opposite arrows is a bond f_{dipz}. The large open circles attached to part of the field points are statistical weights W_r.

C. Integrability of the prototype P diagrams

The integrability of the prototype P diagrams at short distances can be dealt with as in Sec. IV C when studying the Π graphs. At large distances the bonds f_{Dz} and $\lambda_{\alpha_i}\xi_i\cdot\nabla_i f_{Dz}$ do not cause any trouble since they decay exponentially fast. *A priori*, one has to be more cautious with the bonds f_{dipz}, f_{Rz}, and f_{Rz}^T, which decay algebraically as $1/r^3$. When two clusters of points are separated by a distance R, the product $(\prod F_z)_P$ may now decay only as $1/R^3$ because of the possible presence of articulation points. Consequently, this configuration leads to conditionally convergent integrals.

The way in which these integrals must be calculated could be found by analyzing the behavior of the boundary contributions, all of which vanish in the infinite volume in agreement with the existence of the thermodynamic limit. In fact, this problem is similar to that of the convergence of the coefficients of the fugacity expansions for the classical two-dimensional two-component plasma [34]. The analysis carried out in this case by Speer [34] strongly suggests that one must perform first the integrations over the relative positions of the points belonging to each of the above clusters, then the functional integrations over the shapes of all the filaments except over that of the root point, and third the angular integration over the orientation of $\mathbf{R}$. Then, the remaining integrand decays in fact faster than $1/R^3$ for the following reasons.

Let us consider the two filaments which appear in the $1/R^3$-decaying bond. We call $\mathcal{E}_0$ the filament which is in the same cluster as the root point $\mathcal{E}$, and $\mathcal{E}_i$ the other one. $\mathcal{E}_0$ may be either an internal point or the root point itself. After the integration over the internal points in the cluster, the *a priori* $1/R^3$-decaying term in the large-R expansion of the integrand takes the general form

$$\text{const}\times\int d\Omega_{\mathbf{R}} H(\xi_0)\int \mathcal{D}(\xi_i)K(\xi_i)f_3(\mathbf{R},\xi_0,\xi_i), \quad (5.10)$$

where $d\Omega_{\mathbf{R}}$ is the integration measure over the orienta-

tion of the vector $\mathbf{R}$. An extra integration over ξ_0 is performed only if $\mathcal{C}_0$ is different from the root point. Since $\mathcal{C}_i$ belongs to the cluster where all the variables, except ξ_i and $\mathbf{r}_i$, are integrated over, $K(\xi_i)$ is invariant under the rotations of ξ_i whereas $H(\xi_0)$ is not invariant under those of ξ_0. f_3 denotes the asymptotic parts of either f_{dipz}, f_{Rz}, or f_{Rz}^T, which involve the following $1/R^3$-decaying terms,

$$\lambda_{\alpha_0}\lambda_{\alpha_i}\int_0^1 ds\int_0^1 ds'[\xi_0(s)\cdot\nabla][\xi_i(s')\cdot\nabla]\left[\frac{1}{R}\right], \tag{5.11}$$

$$\int_0^1 ds[\lambda_{\alpha_0}\xi_0(s)\cdot\nabla-\lambda_{\alpha_i}\xi_i(s)\cdot\nabla]^2\left[\frac{1}{R}\right], \tag{5.12}$$

$$\lambda_{\alpha_0}\int_0^1 ds\frac{1}{R}\xi_0(s)\cdot\nabla\left[\frac{1}{R}\right]. \tag{5.13}$$

Because of the rotational invariance of the Gaussian measure $\mathcal{D}(\xi)$, after functional integration the odd terms in the ξ_m's corresponding to the internal points cancel out, while the terms $[\xi_m(s)\cdot\nabla]^2(1/R)$ become proportional to $\nabla^2(1/R)$ when the other part of the integrand is invariant under rotation of ξ_m. The harmonicity of the Coulomb potential then implies that the latter terms are in fact short ranged. Thus, after integration over ξ_i, (5.11) vanishes while the long-range part of (5.12) involves only $\int_0^1 ds[\lambda_{\alpha_0}\xi_0(s)\cdot\nabla]^2(1/R)$. Since $[\xi_0(s)\cdot\nabla]^2(1/R)=2[\xi_0(s)]^2P_2(\cos\theta)/R^3$, where θ is the angle between $\xi_0(s)$ and $\mathbf{R}$, this term vanishes upon integration over the direction of $\mathbf{R}$, for any given $\xi_0(s)$, by virtue of the orthogonality of the Legendre polynomials $P_n(\cos\theta)$. The integration over the orientation of $\mathbf{R}$ also cancels (5.13). Consequently, the integration procedure considered does ensure the convergence of all the P diagrams, as expected.

D. Small-fugacity behavior of the P diagrams

The analysis of the small-z behavior of the P diagrams is complicated by the dependence of the resummed bonds on the fugacities. The bonds f_{Dz}, $\lambda_{\alpha_i}\xi_i\cdot\nabla_i f_{Dz}$, and f_{dipz} are entirely scaled by κ_z^{-1}, while the bonds f_{Rz} and f_{Rz}^T are controlled not only by κ_z^{-1}, but also by the temperature-dependent lengths $\beta e_\alpha e_\gamma$ (Landau length) and λ_α (de Broglie wavelength). The occurrence of various length scales in the resummed bonds prevents simple evaluation of the spatial integrals based on the variable changes $\mathbf{r}_i=\kappa_z^{-1}\mathbf{x}_i$.

In order to disentangle these scales, it is convenient to rewrite $f_{Rz}(\xi_i,\xi_j;\mathbf{r})$, with $\mathbf{r}=\mathbf{r}_i-\mathbf{r}_j$ and $\mathbf{x}=\kappa\mathbf{r}$, as

$$f_{Rz}(\xi_i,\xi_j;\mathbf{r})=f_T(\xi_i,\xi_j;\mathbf{r})+f_T(\xi_i,\xi_j;\mathbf{r})\sum_{n=1}^{\infty}\kappa_z^n H_n(\xi_i,\xi_j;\mathbf{x})+\sum_{n=2}^{\infty}\kappa_z^n G_n(\xi_i,\xi_j;\mathbf{x}), \tag{5.14}$$

where the functions H_n and G_n can be calculated from (4.14) by expanding $\exp(-\beta_{ij}\psi_{\text{chain}})$ in powers of ψ_{chain}. For instance, we find

$$H_1(\xi_i,\xi_j;\mathbf{x})=-\beta_{ij}\frac{[e^{-x}-1]}{x}, \tag{5.15}$$

$$G_2(\xi_i,\xi_j;\mathbf{x})=\frac{\beta_{ij}^2}{2}\frac{e^{-2x}}{x^2}, \tag{5.16}$$

$$G_3(\xi_i,\xi_j;\mathbf{x})=\frac{\beta_{ij}^3}{6}\frac{[1-e^{-3x}]}{x^3}+\beta_{ij}^2\int_0^1 ds[\lambda_{\alpha_i}\xi_i(s)\cdot\hat{\mathbf{x}}-\lambda_{\alpha_j}\xi_j(s)\cdot\hat{\mathbf{x}}]\times\frac{[1-(1+x)e^{-2x}]}{x^3}, \tag{5.17}$$

where $\hat{\mathbf{x}}=\mathbf{x}/|\mathbf{x}|$. The corresponding decomposition of f_{Rz}^T follows immediately by inserting (5.14) into (5.9) and has the same structure as (5.14) with function H_n^T and G_n^T. In fact, H_n^T is reduced to H_n for any n, while only the first three functions G_n^T are different from the corresponding G_n's, i.e., $G_n^T=G_n$ for $n\geq 5$ (in particular G_2^T vanishes). The functions $G_n(x)$ and G_n^T are integrable at large distances as the functions $H_n(x)$ for $n\geq 4$, since they decay at most as $1/x^n$ for x large. The truncated bond f_T does not depend on κ_z^{-1} and is scaled by the above temperature-dependent lengths. The above decompositions of f_{Rz} and f_{Rz}^T with respect to the various scales are quite useful for our purpose, because each term decays at least as $1/r^3$ at large distances. Consequently, use of these decompositions in a given P diagram provides a representation of P as a sum of integrals I_P^{scaled}, the integrands of which are products of functions $f_T(\xi,\xi';\mathbf{r})$ by functions scaled by κ_z^{-1} with the generic form $\kappa_z^p\phi(\xi,\xi';\mathbf{x})$ (where p is a natural integer).

The small-z behavior of I_P^{scaled} is not easy to analyze in real space, because, in general, a given point appears in the arguments of functions controlled by various scales. In order to circumvent this difficulty, we introduce the Fourier transforms

$$\hat{f}_T(\xi,\xi';\mathbf{k})=\int d\mathbf{r}\,e^{i\mathbf{k}\cdot\mathbf{r}}f_T(\xi,\xi';\mathbf{r}), \tag{5.18}$$

$$\tilde{\phi}(\xi,\xi';\mathbf{u})=\int d\mathbf{x}\,e^{i\mathbf{u}\cdot\mathbf{x}}\phi(\xi,\xi';\mathbf{x}), \tag{5.19}$$

and we apply the generalized Plancherel identity. In Fourier space, the integrand of I_P^{scaled} takes the general form

$$\text{const}\times\kappa_z^L\prod W(\alpha,\xi)\prod\tilde{\phi}(\xi,\xi';LC(\{\mathbf{u}\}))\prod\hat{f}_T(\xi,\xi';\kappa_z LC(\{\mathbf{u}\}))\prod\hat{f}_T(\xi,\xi';LC(\{\mathbf{q}\})+\kappa_z LC(\{\mathbf{u}\})), \tag{5.20}$$

where L is an integer while LC is a generic notation for linear combinations of the wave vectors $\mathbf{q}$ or $\mathbf{u}$.

Each function $\hat{f}_T(\xi,\xi';LC(\{\mathbf{q}\})+\kappa_z LC(\{\mathbf{u}\}))$ can be replaced by its Taylor expansion with respect to $\kappa_z LC(\{\mathbf{u}\})$ since $\hat{f}_T(\xi,\xi';\mathbf{k})$ is analytic everywhere except at the origin. Since the large-r expansion of $f_T(\xi,\xi';\mathbf{r})$ only involves inverse integer powers of r starting with $1/r^3$, the small-κ_z expansion of $\hat{f}_T(\xi,\xi';\kappa_z LC(\{\mathbf{u}\}))$ only involves integer powers of κ_z with possible multiplicative $\ln\kappa_z$ factors. Inserting these small κ_z expansions of $\hat{f}_T(\xi,\xi';LC(\{\mathbf{q}\})+\kappa_z LC(\{\mathbf{u}\}))$ and $\hat{f}_T(\xi,\xi';\kappa_z LC(\{\mathbf{u}\}))$ in (5.20), as well as the small-z expansions of the statistical weights $W(\alpha,\xi)$, we obtain a formal representation of I_p^{scaled} as a double integer series in $z^{1/2}$ and $\ln z$. The coefficients of these series are related to the moments of the functions $\tilde{\phi}$, i.e., to

$$\int \prod d\mathbf{u} \prod \tilde{\phi}(\xi,\xi';LC(\{\mathbf{u}\})) \prod [LC(\{\mathbf{u}\})]^p \tag{5.21}$$

and also to

$$\int \prod d\mathbf{q} \prod \hat{f}_T^{(p)}(\xi,\xi';LC(\{\mathbf{q}\})) , \tag{5.22}$$

where the generic notation $\hat{f}_T^{(p)}(\xi,\xi';LC(\{\mathbf{q}\}))$ means a partial derivative of order p with respect to k_μ of $\hat{f}_T(\xi,\xi';\mathbf{k})$. The integrals (5.21) and (5.22) with large values of p diverge in general because the functions $\hat{f}_T^{(p)}(\xi,\xi';\mathbf{k})$ are not integrable at $\mathbf{k}=\mathbf{0}$ and the functions $\tilde{\phi}$ behave algebraically for u large; in real space, the functions ϕ are not analytic functions of $\mathbf{x}^2$ at the origin and some of them are even not integrable at $\mathbf{x}=\mathbf{0}$ because they involve high powers of f_{dipz} which itself diverges as $1/x$ as x goes to zero (the latter divergencies are spurious and have already been discussed in Sec. IV C). However, since only integer powers of u arise in the large-u expansions of $\tilde{\phi}$ and only integer powers of k (apart from possible multiplicative logarithmic terms) arise in the small-k expansion of $\hat{f}_T^{(p)}$, these divergencies should not modify the structure of the small-z expansion of I_P^{scaled} predicted above.

E. Small-fugacity expansion of $\rho_\alpha(\xi)$.

According to the small-z representations of the P diagrams derived in Sec. V D, the functional $\rho_\alpha(\xi)$ can be expanded as

$$\rho_\alpha(\xi)=\sum_{l,n,p} P_\alpha^l(\{z_\gamma^*\}) \left[4\pi\beta\sum_\gamma e_\gamma^2 z_\gamma^*\right]^{n/2} \times \left[\ln\left[\text{const}\times 4\pi\beta\sum_\gamma e_\gamma^2 z_\gamma^*\right]\right]^p \mathcal{F}_\alpha^{l,n,p}(\xi) \tag{5.23}$$

with l,p natural integers and n a relative integer. In (5.23), $P_\alpha^l(\{z_\gamma^*\})$ are homogeneous polynomials of degree l in the fugacities z_γ^* with coefficients depending on the temperature, while the "constants" in the arguments of the logarithmic terms are built with the lengths $\beta e_\gamma e_\delta$ and λ_γ. Moreover, the functionals $\mathcal{F}_\alpha^{l,n,p}(\xi)$ also depend on the temperature.

Now we perform the explicit fugacity expansion of $\rho_\alpha(\xi)$ up to order $z^{3/2}$. First we notice that the weight of a bare point $\mathcal{P}_m$ is exactly $z_{\alpha_m}^*$, whereas the fugacity expansion of the weight of a dressed point $\mathcal{P}_m$ starts as $z^{3/2}$ according to (5.4) and (5.8). Moreover, if $\mathcal{P}_j$ is a bare point which is connected to only one point $\mathcal{P}_i$ by an f_{Dz} bond, then the contribution of this bond is factored as

$$\int d\mathcal{P}_j z_{\alpha_j}^* (-\beta e_{\alpha_i} e_{\alpha_j}) \phi_{Dz}(\mathbf{r}_i-\mathbf{r}_j) = -\frac{4\pi\beta e_{\alpha_i}}{\kappa_z^2}\left[\sum_{\alpha_j} z_{\alpha_j}^* e_{\alpha_j}\right], \tag{5.24}$$

which vanishes because of the constraint (5.1). Without the latter, the above contribution would have been of order z^0 and then an infinity of P diagrams with the above f_{Dz} bonds in them would have contributed to the same order in z.

It is thus straightforward to show that the leading term of the fugacity expansion of $\rho_\alpha(\xi)$ is z_α^*: it arise entirely from the trivial P graph built with the bare root point alone. The next term is of order $z^{3/2}$. It is given by the expansion of the following two diagrams: the single dressed root point and the graph where the root point $\mathcal{E}$ is bare and linked to a dressed point $\mathcal{P}_1$ by an f_{Dz} bond. The sum of the latter graphs reads

$$W_r(\mathcal{E})+z_\alpha^*\left[-\frac{4\pi\beta e_\alpha}{\kappa_z^2}\right]\sum_{\alpha_1} z_{\alpha_1}^* e_{\alpha_1}\int \mathcal{D}(\xi_1) W_r(\alpha_1,\xi_1) \tag{5.25}$$

and the leading term of its fugacity expansion is given by replacing $W_r(\mathcal{P}_m)$ by the first term of $z_{\alpha_m}^* I_r(\mathcal{P}_m)$ with the result

$$g_\alpha^{(3/2)}(\{z_\gamma^*\})=z_\alpha^*\left[\frac{\beta}{2}e_\alpha^2\kappa_z-2\pi\beta^2 e_\alpha\frac{\sum_{\alpha_1} z_{\alpha_1}^* e_{\alpha_1}^3}{\kappa_z}\right]. \tag{5.26}$$

Thus the explicit form of $\rho_\alpha(\xi)$ up to the order $z^{3/2}$ is

$$\rho_\alpha(\xi)=z_\alpha^*+g_\alpha^{(3/2)}(\{z_\gamma^*\})+g_\alpha^{(2)}(\{z_\gamma^*\},\xi)+R_\alpha^{(5/2)}(\{z_\gamma^*\},\xi) , \tag{5.27}$$

where $g_\alpha^{(2)}(\{z_\gamma^*\},\xi)$ is the term of order z^2 in (5.23) and $R_\alpha^{(5/2)}(\{z_\gamma^*\},\xi)$ is the remaining part in (5.23) which starts at the order $z^{5/2}$. We notice that the shape dependence of $\rho_\alpha(\xi)$ does not appear until order z^2 at least.

The fugacity expansion of the particle densities directly follows from (5.23) via functional integrations of the $\mathcal{F}_\alpha^{l,n,p}(\xi)$ with respect to the Gaussian measure $\mathcal{D}(\xi)$. The global structure of (5.23) is unchanged through these integrations, i.e., ρ_α is represented by a double integer series in $z^{1/2}$ and $\ln z$. In particular, the expansion of ρ_α up to the order $z^{3/2}$ coincides with (5.27) since $\rho_\alpha(\xi)$ does not depend on ξ at this order, i.e.,

$$\rho_\alpha=z_\alpha^*+g_\alpha^{(3/2)}(\{z_\gamma^*\})+\int\mathcal{D}(\xi)[g_\alpha^{(2)}(\{z_\gamma^*\},\xi)+R_\alpha^{(5/2)}(\{z_\gamma^*\},\xi)] . \tag{5.28}$$

The neutrality rule (2.5) should be satisfied term by term as it can be explicitly checked for the first two terms.

F. Particle-density expansion of $\rho_\alpha(\xi)$

Since ρ_α behaves as z_α^* when all the z's go to zero, the inversion of the above z expansion of ρ_α leads to a similar representation of z_α^*, i.e., a double integer series in $\rho^{1/2}$ and $\ln\rho$. Moreover the corresponding half powers of ρ enter in $\kappa=(4\pi\beta\sum_\alpha e_\alpha^2\rho_\alpha)^{1/2}$. Inserting the ρ expansions of the z's into (5.23), we finally obtain the required expansion of $\rho_\alpha(\xi)$.

$$\rho_\alpha(\xi)=\sum_{l,n,p} Q_\alpha^l(\{\rho_\gamma\})\left[4\pi\beta\sum_\gamma e_\gamma^2\rho_\gamma\right]^{n/2} \times\left[\ln\left[\text{const}\times 4\pi\beta\sum_\gamma e_\gamma^2\rho_\gamma\right]\right]^p \mathcal{G}_\alpha^{l,n,p}(\xi)\ , \tag{5.29}$$

which has the same structure as (5.23). The polynomials Q_α^l and the functionals $\mathcal{G}_\alpha^{l,n,p}(\xi)$ are related to the P_α^l's and to the $\mathcal{F}_\alpha^{l,n,p}(\xi)$'s. The explicit derivation of these relations is not easy to carry out in general.

Of course, the leading term in (5.29) is nothing but the particle density of species α itself. The identity $\rho_\alpha=\int D(\xi)\rho_\alpha(\xi)$ along with the fact that the first ξ-dependent term in the z expansion of $\rho_\alpha(\xi)$ is of order z^2 imply that the next correction is of order ρ^2 and only involves the shape-dependent part of the z^2 term in (5.27). A straightforward elimination of z in favor of ρ by using (5.28) permits rewriting (5.27) as

$$\rho_\alpha(\xi)=\rho_\alpha+\left[g_\alpha^{(2)}(\{\rho_\gamma\},\xi)-\int\mathcal{D}(\xi')g_\alpha^{(2)}(\{\rho_\gamma\},\xi')\right] +O(\rho^{5/2})\ . \tag{5.30}$$

By inspection of the small-fugacity behavior of the P graphs, the ρ^2 term in (5.30) is found to be given by the expansion of the graph where the bare root point is linked to a bare point $\mathcal{P}_1$ by a f_{Rz}^T bond, with the result

$$\rho_\alpha(\xi)=\rho_\alpha+\sum_\gamma\rho_\alpha\rho_\gamma\int d\mathbf{r}\int\mathcal{D}(\xi_1)\left[f_T(\xi,\xi_1;\mathbf{r})-\int\mathcal{D}(\xi')f_T(\xi',\xi_1;\mathbf{r})\right]+O(\rho^{5/2})\ . \tag{5.31}$$

According to the definition (4.2) of f_T, after integration over ξ_1, f_T can be replaced by f in the integrand of (5.31). Therefore the first two terms in (5.29) are merely calculated as

$$\rho_\alpha(\xi)=\rho_\alpha+\sum_\gamma\rho_\alpha\rho_\gamma\int d\mathbf{r}\int\mathcal{D}(\xi_1)\left[\exp\left[-\beta e_\alpha e_\gamma\int_0^1 ds\, v_C[|\mathbf{r}+\lambda_\gamma\xi_1(s)-\lambda_\alpha\xi(s)|]\right]\right.$$
$$\left.-\int\mathcal{D}(\xi')\exp\left[-\beta e_\alpha e_\gamma\int_0^1 ds\, v_C[|\mathbf{r}+\lambda_\gamma\xi_1(s)-\lambda_\alpha\xi'(s)|]\right]\right]+O(\rho^{5/2})\ . \tag{5.32}$$

The structure of the ρ^2 term in (5.32) is identical to that for a system with short-range forces. In other words, no screening mechanism is needed for ensuring the finiteness of the corresponding integral, the integrand of which indeed decays a $1/r^4$ after integration over the angles of $\mathbf{r}$. The first nonanalytic term in (5.32) which is induced by the long-range nature of the Coulomb potential is of order $\rho^{5/2}$. Contrarily to the ρ^2 term, the latter results in part from screening effects and consequently makes κ appear. Eventually, we notice that the identity $\rho_\alpha=\int\mathcal{D}(\xi)\rho_\alpha(\xi)$ implies that each corrective term to ρ_α in (5.32) must be such that its integral over ξ vanishes. The ρ^2 term obviously exhibits this property.

ACKNOWLEDGMENT

The Laboratoire de Physique is "Unité de Recherche Associée au CNRS No. 1325." The Laboratoire de Physique Théorique–ENSLAPP is "Unité de Recherche Associée au CNRS No. 1436."

APPENDIX

In order to prove the relation (4.6) we have to go back to the formulation of diagrammatics with labeled diagrams as Meeron did in Ref. [10]. The relation between the formulations with either unlabeled $\tilde{\Gamma}$ diagrams or labeled $\tilde{\Gamma}_N$ diagrams (where N is the number of internal points of the diagram $\tilde{\Gamma}_N$) is the following:

$$h(\mathcal{C}_a,\mathcal{C}_b)=\sum_{\tilde{\Gamma}}\frac{1}{S_{\tilde{\Gamma}}}\int\prod_{i=n}^N d\mathcal{C}_n\rho(\mathcal{C}_n)\left[\prod\tilde{f}\right]_{\tilde{\Gamma}} =\sum_{N=0}^\infty\frac{1}{N!}\int\prod_{i=n}^N d\mathcal{C}_n\rho(\mathcal{C}_n)\sum_{\text{labeled }\tilde{\Gamma}_N}\left[\prod\tilde{f}\right]_{\tilde{\Gamma}_N}\ . \tag{A1}$$

Every diagram $\tilde{\Gamma}_N$ leads to a prototype diagram Π_M with M internal points $\mathcal{P}_i$'s ($M\le N$) when all its Coulomb points are suppressed and $[\prod\tilde{f}]_{\tilde{\Gamma}_N}$ can be factored as $\prod_{\{ij\}\text{ bonds}}[\prod\tilde{f}]_{\tilde{\Gamma}_{ij}}$, where $\tilde{\Gamma}_{ij}$ is the part of the diagram $\tilde{\Gamma}_N$ which connects $\mathcal{P}_i$ to $\mathcal{P}_j$ directly and/or by products of Coulomb chains. If we first integrate over the Coulomb points we have to choose the labels for the M $\mathcal{P}_m$'s and for the n_{ij} Coulomb points $\mathcal{C}_k^{\{ij\}}$'s of every $\tilde{\Gamma}_{ij}$. The number of ways of choosing M labels among N is $N!/(N-M)!M!$ and the number of ways of choosing the n_{ij} labels for each pair $\{ij\}$ among $N-M$ labels is $(N-M)!/\prod_{\{i,j\}}n_{ij}!$, so

$$h(\mathcal{C}_a,\mathcal{C}_b)=\sum_{N=0}^{\infty}\frac{1}{N!}\sum_{M=0}^{N}\frac{N!}{(N-M)!M!}\int\prod_{m=1}^{M}d\mathcal{P}_m\rho(\mathcal{P}_m)\sum_{\text{labeled }\Pi_m}\sum_{\{n_{ij}\}}\frac{(N-M)!}{\prod_{\{i,j\}}n_{ij}!}\prod_{\{ij\}\text{ bonds}}\int\prod_{k=1}^{n_{ij}}d\mathcal{C}_k^{\{ij\}}\rho(C_k^{\{ij\}})\times\sum_{\text{labeled }\bar{\Gamma}_{ij}}\left[\prod\tilde{f}\right]_{\bar{\Gamma}_{ij}},\tag{A2}$$

where $\sum_{\{n_{ij}\}}$ is the sum over all sets of n_{ij}'s which satisfy $\sum_{\{i,j\}}n_{ij}=N-M$. Now the summation over N can be eliminated and the constraint over $\sum_{\{i,j\}}$ vanishes with the result

$$h(\mathcal{C}_a,\mathcal{C}_b)=\sum_{M=0}^{\infty}\frac{1}{M!}\int\prod_{m=1}^{M}d\mathcal{P}_m\rho(\mathcal{P}_m)\sum_{\text{labeled }\Pi_M}\left[\prod_{\{ij\}\text{ bonds}}F(\mathcal{P}_i,\mathcal{P}_j)\right]\tag{A3}$$

with the definition

$$F(\mathcal{P}_i,\mathcal{P}_j)=\sum_{n_{ij}=0}^{\infty}\frac{1}{n_{ij}!}\int\prod_{k=1}^{n_{ij}}d\mathcal{C}_k^{\{ij\}}\rho(\mathcal{C}_k^{\{ij\}})\sum_{\text{labeled }\bar{\Gamma}_{ij}}\left[\prod\tilde{f}\right]_{\bar{\Gamma}_{ij}}.\tag{A4}$$

Coming back to the formulation with unlabeled diagrams we get

$$h(\mathcal{C}_a,\mathcal{C}_b)=\sum_{\Pi}\frac{1}{S_\Pi}\int\prod_{m=1}^{M}d\mathcal{P}_m\rho(\mathcal{P}_m)\left[\prod F\right]_\Pi\tag{A5}$$

with

$$F(\mathcal{P}_i,\mathcal{P}_j)=\sum_{\bar{\Gamma}_{ij}}\frac{1}{S_{\bar{\Gamma}_{ij}}}\int\prod_{k=1}^{n_{ij}}d\mathcal{C}_k^{\{ij\}}\rho(\mathcal{C}_k^{\{ij\}})\left[\prod\tilde{f}\right]_{\bar{\Gamma}_{ij}}.\tag{A6}$$

[1] Ch. Fefferman, Rev. Math. Iberoam. **1**, 1 (1985)

[2] J. E. Mayer and M. G. Mayer, *Statistical Mechanics* (Wiley, New York, 1940); J. E. Mayer and E. Montroll, J. Chem. Phys. **9**, 2 (1941).

[3] See, e.g., J. Ginibre, in *Statistical Mechanics and Quantum Field Theory,* 1971 Les Houches Lectures, edited by C. de Witt and R. Stora (Gordon and Breach, New York, 1971).

[4] See, e.g., B. Simon, *Functional Integration and Quantum Physics* (Academic, New York, 1979).

[5] J. E. Mayer, J. Chem. Phys. **18**, 1426 (1950).

[6] E. E. Salpeter, Ann. Phys. (N.Y.) **5**, 183 (1958).

[7] G. Gouy, J. Phys. Théor. Appl. **9**, 457 (1910); Ann. Phys. (Paris) **7**, 129 (1917).

[8] D. L. Chapman, Lond. Edinb. Dubl. Philos. Mag. **25**, 475 (1913).

[9] P. Debye and E. Hückel, Z. Phys. **24**, 185 (1923).

[10] E. Meeron, J. Chem. Phys. **28**, 630 (1958); *Plasma Physics* (McGraw-Hill, New York, 1961).

[11] R. Abe, Prog. Theor. Phys. **22**, 213 (1959).

[12] W. Ebeling, Ann. Phys. (Leipzig) **19**, 104 (1967).

[13] W. Ebeling, W. D. Kraeft, and D. Kremp, *Theory of Bound States and Ionization Equilibrium in Plasmas and Solids* (Akademie-Verlag, Berlin, 1976).

[14] W. D. Kraeft, D. Kremp, W. Ebeling, and G. Röpke, *Quantum Statistics of Charged Particle Systems* (Plenum, New York, 1986).

[15] F. J. Rogers, Phys. Rev. A **10**, 2441 (1974).

[16] See, e.g., A. Fetter and J. D. Walecka, *Quantum Theory of Many-Particles Systems* (McGraw-Hill, New York, 1971).

[17] E. W. Montroll and J. C. Ward, Phys. Fluids **1**, 55 (1958); A. Sakakura, Ph.D. thesis, University of Colorado, 1960; H. E. DeWitt, J. Nucl. Energy C **2**, 27 (1961).

[18] E. H. Lieb and J. L. Lebowitz, Adv. Math. **9**, 316 (1972).

[19] See, e.g., D. Chandler, in *Studies in Statistical Mechanics,* edited by E. W. Montroll and J. L. Lebowitz (North-Holland, Amsterdam, 1981).

[20] D. Brydges and P. Federbuch, in *Rigorous Atomic and Molecular Physics,* Vol. 74 of *NATO Advanced Study Institute, Series B: Physics,* edited by G. Velo and A. S. Wightman (Plenum, New York, 1981); D. Brydges and E. Seiler, J. Stat. Phys. **42**, 405 (1986).

[21] A. Alastuey and Ph. A. Martin, Phys. Rev. A **40**, 6485 (1989); F. Cornu and Ph. A. Martin, *ibid.* **44**, 4893 (1991).

[22] A. Alastuey and A. Perez, Europhys. Lett. **20**, 19 (1992); A. Alastuey, F. Cornu, and A. Perez, in *Strongly Coupled Plasma Physics,* edited by H. M. van Horn and S. Ichimaru (University of Rochester, Rochester, 1993).

[23] This general property of Coulomb systems has been explicitly checked for two-dimensional classical models with logarithmic interactions by F. Cornu and B. Jancovici, J. Chem. Phys. **90**, 2444 (1989); F. Cornu, J. Stat. Phys. **54**, 681 (1989).

[24] For a review see, e.g., E. H. Lieb, Rev. Mod. Phys. **48**, 553 (1976).

[25] F. J. Dyson and A. Lenard, J. Math. Phys. **8**, 423 (1967); A. Lenard and F. J. Dyson, *ibid.* **9**, 698 (1968); see also Ref. [24] for a simple derivation of the H stability.

[26] R. P. Feynman and A. R. Hibbs, *Quantum Mechanics and Path Integrals* (McGraw-Hill, New York, 1965).

[27] T. Morita, Prog. Theor. Phys. Jpn. **22**, 757 (1959).

[28] T. Morita and K. Hiroike, Prog. Theor. Phys. Jpn. **25**, 537 (1961); C. de Dominicis, J. Math. Phys. **3**, 983 (1962); **4**, 255 (1963); G. Stell, in *The Equlibrium Theory of Classical Fluids,* edited by H. L. Frisch and J. L. Lebowitz (Benjamin, New York, 1964).

[29] The two-body bond structure of the Mayer graphs in the FK representation is also a key ingredient in the proofs of convergence of the Mayer series for quantum fluids with short-range forces (see e.g., Ref. [3]).

[30] This bond has been omitted in the proceeding quoted in Ref. [22].

[31] Some shapes $\xi(s)$ make f diverge exponentially fast at the origin. However, the corresponding ensemble has a zero measure. In other words, f is regular at $\mathbf{r}=\mathbf{0}$ for most shapes. This point has been rigorously proved in Ref. [4].

[32] M. Lavaud, J. Stat. Phys. **19**, 429 (1978).

[33] The same mechanism ensures the integrability of the Mayer graphs for classical dipolar fluids, as shown by G. Stell, in *Modern Theoretical Chemistry,* edited by B. J. Berne (Plenum, New York, 1977), Vol. 5; D. Chandler, J. Chem. Phys. **67**, 1113 (1977).

[34] E. R. Speer, J. Stat. Phys. **42**, 895 (1986).